THE ASTROPHYSICAL JOURNAL

AN INTERNATIONAL REVIEW OF SPECTROSCOPY AND ASTRONOMICAL PHYSICS

VOLUME LXXVIII DECEMBER 1933 NUMBER 5

A MODIFICATION OF THE SCHILT PHOTOMETER FOR THE MEASUREMENT OF STELLAR MAGNITUDES FROM PHOTOGRAPHS

By ARTHUR L. BENNETT

ABSTRACT

An instrument built in the Yale University Observatory shop is described and illustrated. The photographic plate is mounted horizontally. The Weston photronic cell is used as the light-sensitive element, in conjunction with a galvanometer. The field of the plate being measured, the galvanometer scale and the two co-ordinate scales are brought into a single eyepiece.

An instrument for the measurement of stellar magnitudes from photographs has recently been completed in the Yale Observatory shop. The optical arrangement follows in general that of the instrument designed by Schilt.[1] There are, however, two major changes: first, the photographic plate is mounted horizontally instead of vertically; and, second, the Weston photronic cell is used as the light-sensitive element in place of the thermopile.

There are several advantages in mounting the photographic plate horizontally. It is much easier to obtain a rugged and stable construction of the double motion of the plate and at the same time the instrument is made more simple. The photronic cell is cheap and sturdy. Its advantages over the thermopile are that its maximum sensitivity when used with an incandescent lamp as source lies in the visual region and that it is free from thermal disturbances.

Figure 1 is a diagram of the optical system of the photometer.

[1] *Bulletin of the Astronomical Institutes of the Netherlands*, 60, 1924.

Lamp A is the source of light for the measuring beam. An image of its filament is projected on objective F, just below the plate, by condenser B. Objective F throws an image of condenser B on the film of the photographic plate. This image, owing to the short focal length of F, is very much reduced in size and is of great brightness. Diaphragm C serves to reduce the aperture of B, and, consequently, the area of the plate illuminated. Objective H above the plate projects an enlarged image of the plate on diaphragm J. This diaphragm limits the area of the plate to be measured. After passing

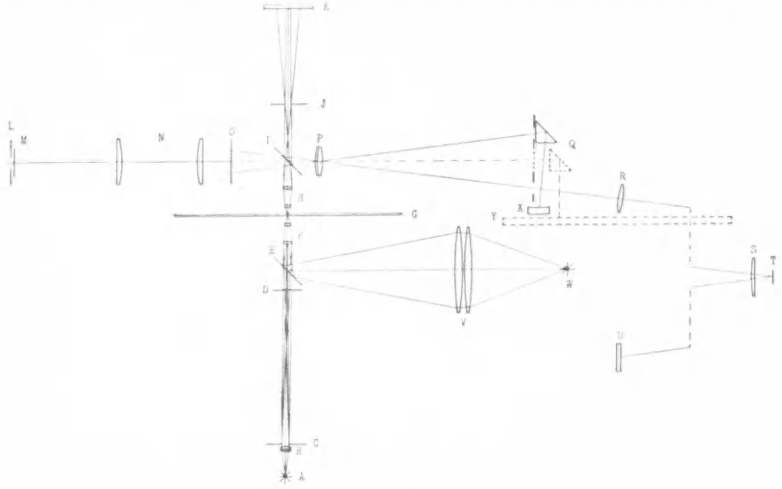

FIG. 1.—The optical system

aperture J, the cone of light spreads out and illuminates a fairly large area of the surface of the photronic cell K.

In order that the part of the plate which is to be measured may be seen, a very thin unsilvered sheet of glass I is used to reflect a part of the beam of light emerging from H at right angles to the axis of the measuring-beam. An image of the plate is thus formed on the cross-wires O, which are at the same distance as diaphragm J from objective H. The cross-wires are viewed through eyepiece N. The area of the plate illuminated by the measuring-beam is much too small for the easy location of the star to be measured. Furthermore, the measuring-beam is too bright for this purpose. Another unsilvered plate E, at 45°, serves to bring in the beam of light from condenser V. This condenser is very much larger than condenser B, so

that a proportionately larger area of the plate is illuminated. Lamp *W* is the source of light for this beam.

In order to eliminate the measuring-beam from the eyepiece, a red Wratten Filter No. 22 is inserted at *D*. This filter absorbs the visual light below λ 5600 without affecting too much the response of the photronic cell (maximum sensitivity at about λ 5800). A green No. 74 filter at *M* passes a narrow band around λ 5300, near the maximum visual sensitivity. The result is that the light of the plate illumination is received by the eye while the measuring-beam is practically suppressed.

The co-ordinate scales *X* and *Y* move with the plate carriage. An image of about 1 cm. of each scale is formed on the cross-wires *O* by means of prisms *Q* and lens *P*. Lens P is very nearly at the same distance from the cross-wires as objective *H*,.so that it does not limit the field of view. An image of the galvanometer scale *U* is formed at *R* by means of lens *S* and the galvanometer mirror *T*. This image also is brought to the cross-wires by lens *P*. Lens *R*, by forming an image of *T* on *P*, produces a field of sufficient size. The areas on condenser *V* which correspond to the positions of the three scales on the cross-wires are blocked out so that the field illumination does not interfere with them. The cross-wires serve as indices for all the scales, which, being reduced by a factor of 3, obstruct only a small area of the image of the plate and are at some distance from the center of the field.

The photographs of the nearly completed instrument (Figs. 2 and 3) show most of the details of construction. The rugged base casting and lower carriage are identical with those used for the blink comparators which had previously been built in the Yale shop. These are made of heavily ribbed cast iron and, consequently, permit a minimum of flexure. The sturdy cast-iron bridge which carries the optical parts above the plate is attached to the base. Rotating in the face of the upper carriage is a duralumir disk which can be turned by the removable pinion and handle for the orientation of the plate. The lower carriage is moved to the right and left by the handle on the left (Fig. 2). The upper carriage is moved at right angles to the motion of the lower one by the handle on the right. A full turn of either of these handles moves the plate approximately 11 mm.

A step is cut around the 8×10 inch aperture in the disk of the up-

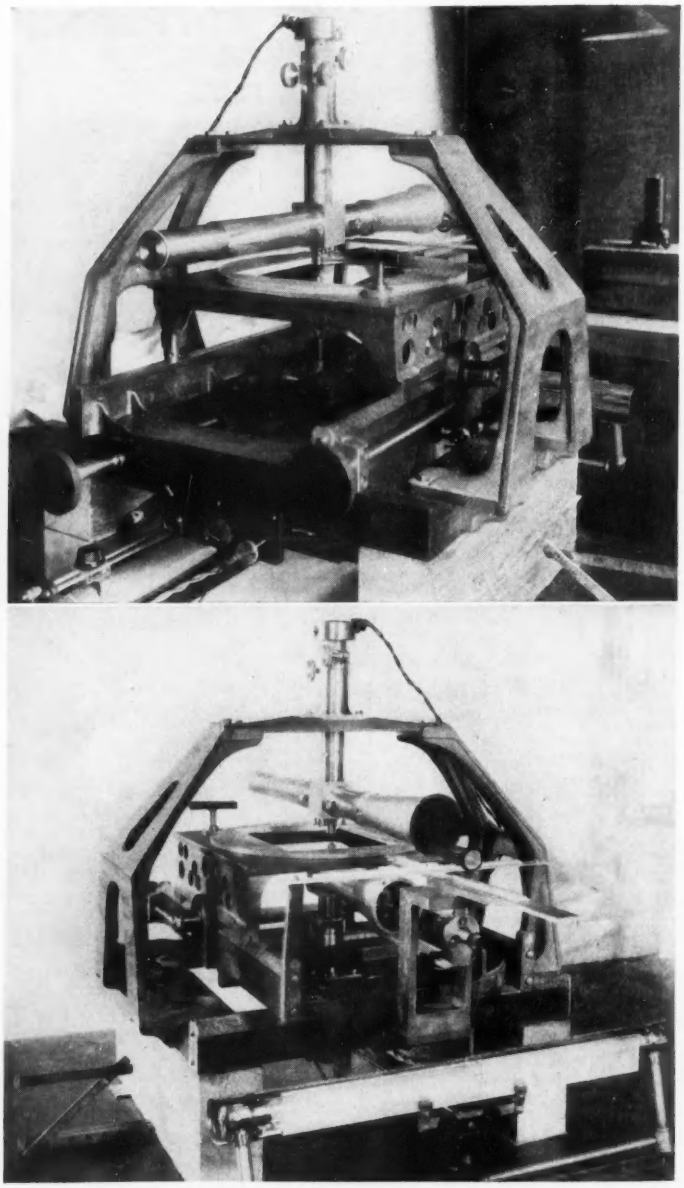

FIGS. 2 (above) and 3 (bottom)

per carriage. The photographic plate is placed in this recess film side down and is held in place by four clamps pressing against the upper side of the plate near the edges. The clamps are not shown in the photographs.

The crosswise or X-scale is easily visible in Figure 3. It is supported from the lower carriage by two brackets and moves with this carriage. A much more complicated arrangement is necessary for the Y-scale. The scale itself is mounted on a metal strip, which slides lengthwise in gibs supported from the base casting. At the inner end of the strip a small roller projects downward into a slot running transversely across the upper face of the upper carriage. The upper carriage is, therefore, free to move transversely. The Y-scale is moved only when the upper carriage is moved on the lower carriage.

The galvanometer scale, seen in the foreground of Figure 3, is a Leeds and Northrup 500-mm. scale graduated on ground glass. It is supported on a metal stand equipped with a rack and pinion for zero adjustment. By means of a universal joint and rod this adjustment is made accessible to the observer. It is controlled by the knurled button to the right below the base casting (Fig. 2). The scale is illuminated by two 11-inch tubular show-case lamps immediately behind it. Semicylindrical reflectors concentrate the light on the scale and also shade the observer.

All of the optical parts are carried on two tubes perpendicular to the plane of the plate. Each tube is supported by a long cylindrical guide. The upper guide can be moved a short distance parallel to the plate in the Y direction, and the lower one in the X direction so that the axes of the two tubes may be accurately collimated. This adjustment is made once for all when the instrument is assembled. For focusing, each tube can be moved parallel to its axis by a rack and pinion and then clamped securely in place. Sufficient movement is provided for the accommodation of either 16-mm or 48-mm objectives. At the end of each tube toward the plate is a cast hollow cube which serves as a support for the tubes parallel to the plate. The objectives screw directly into the faces nearest the plate.

The diaphragm J (Fig. 1) is mounted within the upper tube. An eccentric disk which can be rotated from the outside has a series of seven graded apertures. As each hole reaches the axis, a spring

catch holds the disk in position. The largest aperture corresponds to 0.4 mm on the plate with the 16-mm objective, and the other holes decrease in diameter by approximately the square root of 2. With the 48-mm objectives the diameter of the area measured can be increased to approximately 2 mm.

This diaphragm and the upper objective define the axis of collimation of the measuring-beam. The elements of the lamp unit *A*, *B*, and *C* are made adjustable so that they can be brought accurately into this axis. This unit, on the lower end of the lower tube beneath the base casting, cannot be seen in the photographs. The iris diaphragm *C*, the shutter, and the condensing lens *B* are mounted together on a plate which can be moved in two directions perpendicular to the axis of the beam and to each other by means of screws with knurled heads. The lamp *A* is guided parallel to the axis for focusing and is held in position by a knurled clamp screw. It also is provided with a double slow motion in the plane parallel to the plate.

The photronic cell fits into a metal cup on the top of the upper tube and is held in position by a knurled-head screw.

The eyepiece tube slides into a larger one secured to the side of the upper cube. On the side of this tube is a knurled-head screw, attached to a short inside tube on which are mounted the cross-wires. This screw serves as a handle and clamp for moving the cross-wires and locking them in position. The wires can be rotated about the axis of the tube to make them parallel to the motions of the image of the plate and can also be moved to and from the cube.

On the opposite side of the upper cube is a similar knurled head which serves to focus the lens *P*. The tube on this side is extended as a support for the prisms *Q* and the arm which carries the lens *R*.

A microscope cover-glass is mounted on a frame within the upper cube to reflect the image of the plate into the eyepiece. This frame is held by springs against the three knurled-head screws which project through the face nearest to the plate.

The condensing lens for the field illumination is supported by a conical tube attached to the lower cube. An arm projecting beyond the lens carries the lamp, which can be moved in three directions for focusing and collimation. Another cover-glass within the lower cube is mounted in a manner similar to that of the one within the upper cube.

The galvanometer can be seen in the background of Figure 2. The Leeds and Northrup 2500*e* Type R was chosen for several reasons: it is moderate in price, has a short period (3 sec.), and is well fitted for use in a circuit with the photronic cell. From the data at hand when the instrument was designed, it appeared that the internal resistance of the photronic cell would vary rather widely for the range of illumination to be used.[2] A galvanometer circuit was planned, therefore, in which a shunt across the galvanometer several times smaller than the internal resistance of the cell would furnish most of the damping resistance and thus minimize the change in damping due to the change in internal resistance. At the same time this damping resistance should be several times larger than the internal resistance of the galvanometer in order that the sensitivity should not be decreased too seriously. The galvanometer has a critical damping resistance of 2400 ohms and an internal resistance of 500 ohms. Since the "dark" resistance of the photronic cell is of the order of 7000 ohms, this galvanometer fills the requirements very well. It was found that the damping was practically the same at full-scale deflection as with the cell dark.

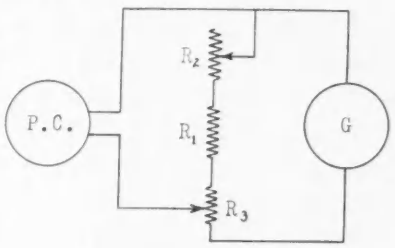

FIG. 4.—Galvanometer circuit

The circuit used is shown in Figure 4. R_1 is a fixed resistance of 1500 ohms, R_2 a 2000-ohm rheostat for the adjustment of the damping, and R_3 a 200-ohm potentiometer. The latter provides a very smooth and fine adjustment over a range of approximately 10 per cent of the maximum sensitivity. Ordinary radio resistances are used. The controls can be seen in Figure 2, at the finger-tips of the observer. The tubular rheostat beneath the instrument is used to vary the lamp voltage for the rough adjustment of the deflection for clear film. The fine adjustment is made by varying the galvanometer sensitivity.

The sensitivity, although not quite as high as might be wished, is

[2] According to the investigation of B. P. Romain (*Review of Scientific Instruments*, 4, 83, 1933), the internal resistance of the photronic cell would change only 1 or 2 per cent over the range of illumination used here.

ample for the ordinary use of the instrument. With a 32-c-p. automobile headlight lamp and the 16-mm objectives, the deflection is well over 500 mm at 1.5 m for an area on the clear film of the plate 0.2 mm in diameter. The galvanometer response is very nearly proportional to the amount of light transmitted by the plate.

The collimation and focusing of the instrument are very simply performed. The lower objective is unscrewed and the image of the filament of the lamp *A* focused in the plane of the back lens of the objective. The photronic cell is removed and a fitting put in its place which holds a tube coaxial with and inside of the upper tube of the instrument. At the lower end of this auxiliary tube is a 48-mm objective which serves to project an image of the diaphragm *J* upon the ceiling or a screen. The upper tube is then moved by means of the rack and pinion until the grain of the plate, or a star image, is also sharply focused. The iris diaphragm *C* is now closed until its edge becomes visible and the lower tube moved until the iris is brought into focus. The iris is opened and a star image set to the center of diaphragm *J*. It is then closed so that its image is smaller than that of *J*, and is now collimated by moving it until its image is centered on that of the star. The iris is finally opened so that its image is just slightly larger than that of diaphragm *J*. The adjustment of the measuring-beam is completed by collimating the lamp filament. This is done by moving it until maximum brightness on the screen, or better, maximum deflection of the galvanometer, is secured.

The cross-wires are next adjusted. The star image is then brought to their intersection by means of the adjusting screws which move the reflecting plate within the upper cube. The reflecting plate within the lower cube is set to center the image of the condenser *V* on the cross-wires and the lamp *W* is focused and collimated. These latter adjustments are permanent. The lens *P* is focused so as to bring the image of the co-ordinate scales to the cross-wires; and, finally, the galvanometer scale is moved until its image is in focus.

Much credit is due to Mr. August Klocker, mechanician at the Observatory, for working out many of the mechanical details and for the excellence with which the instrument was constructed.

YALE UNIVERSITY OBSERVATORY
June, 1933

PHOTOMETRY WITH THE SCHRAFFIERKASSETTE[1]

By WILLIAM H. CHRISTIE

ABSTRACT

The new Schraffierkassette constructed in the Observatory shops is described in detail and the method of measuring and reducing the plates obtained with it is briefly outlined.

Although the Schraffierkassette or, to call it by the accepted English name, the moving-plate camera, was described by Meyermann and Schwarzschild about twenty-five years ago,[2] this effective device does not seem to have become as well known as it deserves. Some time ago the writer designed an instrument with an oscillating plate-base, which has since been constructed in the Observatory shops, for the investigation of variable stars, clusters, and nebulae with the 10-inch Cooke refractor and the 100-inch reflector. Sufficient work has now been done with the instrument to show that it fulfils every expectation, and that photometric observations made with it are surpassed in accuracy only by those made with the photoelectric photometer in capable hands. Since even a modest astrographic camera becomes a powerful instrument for photometric studies when equipped with such a device, it seems desirable to describe the instrument and the method of measuring the plates made with it in some detail, especially since our design differs considerably from that of the instrument described in the aforementioned papers.

With the ordinary methods of procedure the photographic plate falls considerably short of what it is ~~inherently~~ capable. This failure is due, principally, to two sources of error: first, to the small local irregularities in the sensitiveness and distribution of the silver grains; and, second, to the lack of perfection of the optical parts of the instrument. By making the images of the stars large enough and integrating the density of the whole affected area the effects of small local irregularities practically disappear. This method is, however,

[1] *Contributions from the Mount Wilson Observatory, Carnegie Institution of Washington*, No. 476.

[2] *Astronomische Nachrichten*, **170**, 277, 1906; *ibid.*, **174**, 137, 1907.

not without its disadvantages, for, because of the aberrations of the optical system of the telescope, extra-focal images are seldom of uniform density; moreover, coma destroys the symmetry of images at some distance from the optical axis.

These difficulties can largely be overcome by trailing the focal, or near-focal, image of the star up and down and across the plate. If the motions are uniform and the trails close enough together, a patch of blackened silver grains is built up which is unaffected by the imperfections of the optical system, except at the edge, a small area that can be eliminated during measurement by the use of a suitable diaphragm. The Schraffierkassette thus hatches the photographic plate with the star images, and all the aforementioned defects become inappreciable if the hatched area is sufficiently large.

When the field is large there remains one unavoidable source of error, however, due to the falling-off of the intensity of the light at some distance from the optical axis, and a correction must be made after a careful determination of the coefficient of the diminution of the intensity of the illumination has been made.

The instrument under discussion consists of two rectangular metal frames, one sliding within the other, the motions of the two frames being at right angles to each other. The guides in which these frames move are equipped with ball bearings to reduce friction to a minimum, while strong spiral springs hold the frames against their driving mechanism. Two plate-holder adapters, 4×5 and 5×7 inches, are provided which may be attached to the inner frame by means of four screws. The smaller adapter has a double-slide plate-base in order that a series of exposures may be made on the same plate.

The mechanism of the instrument is shown diagrammatically in Figure 1. *A* is a synchronous motor attached to the base of the instrument; the end of the motor-shaft carries a worm, *B*, which engages with a worm-wheel, *C*, attached to a cam-shaft, *D*. The speed of the motor is 1500 revolutions per minute, which, with a reduction of 50:1 provided by the worm and worm-wheel, turns the cam-shaft at the rate of thirty revolutions per minute. Attached to the cam-shaft is a heart-shaped, uniform-motion cam, *E*, and two diametrically placed actuating studs, *G*.

An extension, *H*, to the inner frame, passing below the outer frame, is pressed against one end of the rocker-arm, *I*, by means of two springs, *JJ*; the other end of the rocker-arm carries a hardened steel roller, *K*, which presses in turn against the uniform-motion cam *E*. The rocker-arm is slotted for part of its length, and the pivot, *L*, on which it turns, passes through this slot and may be clamped in any desired position. The pivot is, in turn, attached to

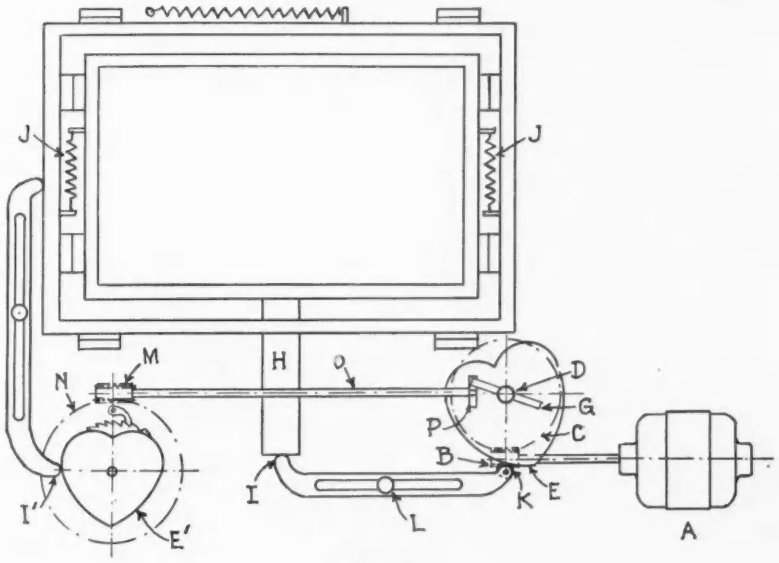

FIG. 1

a small base sliding between gibs parallel to the normal position of the rocker-arm. This arrangement permits the motion of the frame to be adjusted to the desired amplitude.

The outer frame is operated by a second uniform-motion cam and rocker-arm, *E′* and *I′*, similar to the first, the uniform-motion cam being rotated by means of a worm and worm-wheel, *M* and *N*. At the end of the shaft, *O*, carrying the worm, is a Geneva sprocket, *P*, which is operated by the actuating studs, *G*, attached to the first cam-shaft. As the first shaft revolves, the actuating studs give intermittent impulses to the second worm-wheel, and thence, through the uniform-motion cam and a second rocker-arm, to the outer frame.

The second worm-wheel is not fastened to its shaft but is free to turn upon it, motion being transferred from it to the shaft by means of a pawl attached to one face of the worm-wheel and a ratchet-wheel attached to the shaft. A knurled knob at one end of the shaft enables the operator to turn it to the starting position when ready to begin an exposure, eliminating the necessity of waiting until the cam reaches this position with its own motion. A considerable amount of time is saved by this device, especially when a number of short exposures are being made. A contact pin attached to the second cam-shaft closes an electrical circuit about ten seconds before the instrument reaches the starting position and thus operates a small 6-volt flashlight bulb heavily coated with translucent red enamel. The breaking of the circuit is arranged to take place when the outer frame is at the limit of its motion. The flashing-on of the light serves as a warning signal for the operator and provides ample time for him to prepare to open or close the slide as the light flashes off.

The size of the images obtainable with our instrument varies between 0.8 and nearly 5 mm square, the size used depending upon the nature of the investigation. For faint stars it is necessary to use small images in order to keep the exposure times within reasonable limits. For the investigation of the brightness of extended surfaces, such as nebulae and clusters, it is important that the amplitude of the motion of the plate be greater than twice the diameter of the object under investigation in order that all parts of the image may traverse the central region of the square.

The instrument just described is not in its original form. When it was first designed no source of alternating current was available at the 100-inch telescope, and, in order to keep the motor running at a uniform speed, the Gerrish system of control was used, a universal motor taking the place of the present synchronous motor. The control operated as follows: At each swing of an electrically sustained pendulum, beating seconds, an electrical contact was made which closed a relay that, in turn, closed a second relay in the 110-volt motor circuit. These relays remained closed until the low-voltage circuit was broken by means of a circuit-breaker attached to the first cam-shaft, when it remained broken until again closed by the

pendulum. In this manner the motor was kept running at a constant speed, for, if it tended to run too slowly, the circuit was broken after a longer interval, or, if too fast, after a shorter interval than would be the case were the motor running at normal speed. The inertia of a heavy flywheel and the rotor of the motor smoothed out the effects of the intermittent impulses. To start the motor it was necessary to short the circuit-breaker so that the relays would remain closed until the motor attained speed; a switch placed across the leads to the circuit-breaker served this purpose. The Gerrish system of control as applied to the Schraffierkassette is shown schematically in Figure 2.

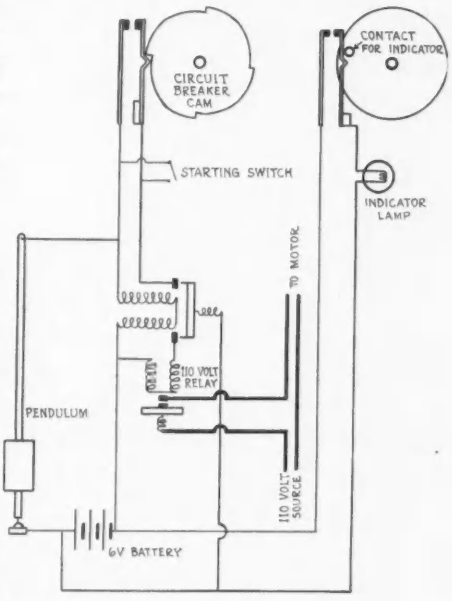

FIG. 2

The experience gained during the construction and operation of this instrument has shown that in order to reduce the effects of errors in cutting the cams they should be made as large as reasonable limits will permit, for, it must be noted, they are not simple Archimedian spirals; the path of the axis of the roller, rolling around the periphery of the cams, should be a true spiral, and it will be found advisable to make these rollers fairly large.

Accurate photometric measurement of the light of bright stars is difficult, owing to the lack of suitable comparison stars. In order to overcome this difficulty small neutral screens have been prepared which may be used to cut down the light of the object under investigation. These screens are about 0.5 inch square and are mounted on small rods which fit into a socket attached to the base of the instrument. The star is centered on the screen, which occupies the central region of the field just in front of the plate-holder; the re-

sulting images can be readily compared with those of the surrounding, fainter stars.

A photograph of the instrument attached to the 10-inch Cooke refractor is shown in Plate IX*a*, and a portion of a photograph of the Pleiades made with this instrument, in Plate IX*b*.

The densities of the images on the plates are measured with a Schilt microphotometer.[3] Our instrument differs in a few minor details from Schilt's machine: It is so mounted that the plate-carrier is horizontal, and for the field illumination a second source of light is used which may be switched off during measurement of the image. A red filter and an opaque screen can be swung into the beam of light falling on the image, the red screen being used when centering the image and the opaque one when reading the zero point.

The galvanometer deflections are read by a scale divided into inches and tenths, mounted about six feet in front of the galvanometer, which is placed as close as possible to the thermocouple mounting in order to keep the leads short. A small plane mirror placed a short distance in front of the telescope reflects the light from the galvanometer mirror into the telescope. With the instrument in proper adjustment, the several readings of the object under measurement, usually four or five, interspersed among the readings of the comparison stars, have an average deviation of about three one-hundredths of an inch.

The thermocouple housing and its supporting frame are wrapped with several layers of cotton batting, which reduces considerably the drift of the zero point; and, by keeping the leads from the thermocouple to the galvanometer short, the drift has been reduced to a negligible amount.

The sensitivity of the instrument is such that with properly exposed and developed plates a scale deflection of five inches corresponds to a difference of about one magnitude; this sensitivity can, of course, be varied by altering the intensity of the light-source and by the use of diaphragms placed between the condensing lens and the plate in the beam of light falling on the image.

When possible, about ten comparison stars, covering a range in brightness greater than that of the variable, are measured, if the

[3] *Bulletin of the Astronomical Institutes of the Netherlands*, **2**, 60, 1924.

PLATE IX

a

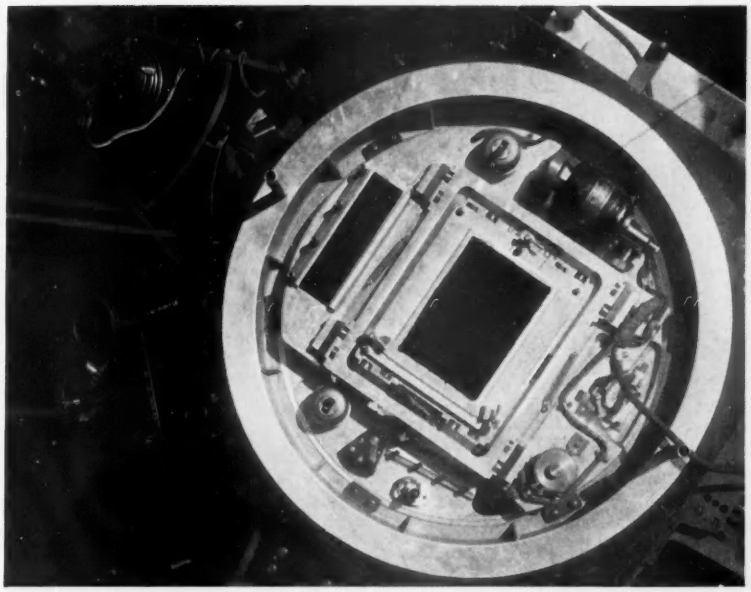

SCHRAFFIERKASSETTE ATTACHED TO THE 10-INCH COOKE REFRACTOR

b

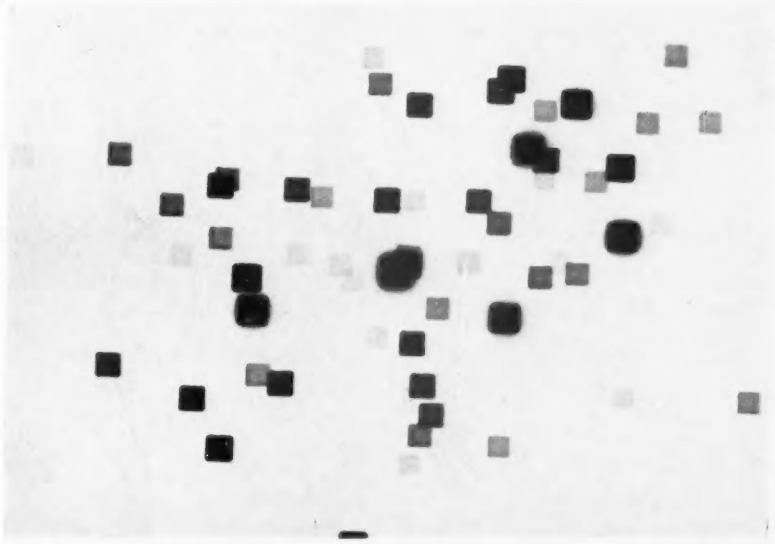

THE PLEIADES PHOTOGRAPHED WITH THE SCHRAFFIERKASSETTE

UNIV. OF MICH.

range of the latter is not too great. The measures of the comparison stars are plotted on an arbitrary magnitude scale on cross-section paper with the galvanometer deflections as abscissae, and a smooth curve, which usually approximates a straight line, is drawn through them; the magnitude of the variable is then read from this arbitrary scale. When a large number of observations of a variable are to be made, it has been found very convenient to construct a permanent ordinate scale of stiff paper on which the brightness of the comparison stars is marked along with the numbers that have been assigned to them. This scale is laid vertically on the cross-section paper and the galvanometer readings plotted as they are read off from the measures. In this manner a plate can be measured and reduced in about fifteen minutes. The arbitrary magnitude scale is later calibrated with the international scale by direct comparison of the field of the variable with the North Polar Sequence. In case the brightness of the variable ranges over an interval of more than one magnitude, one or more additional sets of comparison stars are chosen in order that the range covered be kept small.

With the Imperial Eclipse (Soft) plates, which we have used to a great extent in this work, the opacities of the images are directly proportional to the brightness of the stars over a considerable range, a characteristic which greatly facilitates the reduction of the measures, for the galvanometer deflections are proportional to the magnitudes of the stars for a range of nearly two magnitudes. If the plate has been fully developed, all the reduction-curves made when the stars lie on this portion of the characteristic curve are straight lines.

For an example of the accuracy attained with this instrument the reader is referred to the light-curve of H.D. 198287–8, which appeared in a previous paper.[4]

CARNEGIE INSTITUTION OF WASHINGTON
MOUNT WILSON OBSERVATORY
May 1933

[4] *Mt. Wilson Contr.*, No. 475; *Astrophysical Journal*, **78**, 200, 1933.

MEASUREMENTS OF THE RADIATION FROM VARIABLE STARS[1]

By EDISON PETTIT and SETH B. NICHOLSON

ABSTRACT

Observational data.—The observations were obtained in the usual manner with the vacuum thermocouple at the Newtonian focus of the 100-inch telescope during the interval 1921–1927. The more complete data refer to eleven long-period variables, five irregular variables, two Cepheids, and Algol.

The long-period variables.—Six long-period variables have been observed sufficiently to give curves of radiation at all phases. Their radiometric magnitudes m_r, bolometric magnitudes m_b, water-cell absorptions WC, radiation transmitted by the water cell m_{WC} and that eliminated by the water cell m_W are compared with the visual magnitudes m_v. The mean curves for these six stars show that the maximum intensity of m_{WC} occurs 0.04 phase later than that of m_v; m_r, 0.1 phase later than m_v; and m_W and m_b, 0.14 phase later than m_v. The real energy-maximum, therefore, occurs 50 days later than the light-maximum, at a time when the star is 1.5 mag. fainter than its greatest brightness. The mean variation of m_r is 1.01 mag.; WC, 0.71 mag.; m_{WC}, 1.63 mag.; m_W, 0.92 mag.; m_b, 0.89 mag.; and m_v, 5.9 mag. An additional list of ten long-period variables, observed on a few nights only, shows no abnormal characteristics and indicates that the foregoing results are probably representative for stars of this class.

Temperatures and diameters of long-period variables.—On the average the temperatures range from a minimum of 1800° K to a maximum of 2350° K, the phases agreeing nearly with the corresponding phases of light. The coolest star of type Me so far observed is χ Cygni, which varies from 1630° to 2260° K. The average variation in diameter necessary to explain the observed variation in energy is from 0″.033 to 0″.048, which is 37 per cent of the mean. R Hydrae has the largest maximum diameter, 0″.065. The velocity-curve of o Ceti deduced from the radiometric measures is in phase with what would be expected from the Cepheids, but opposite to the phase observed spectroscopically. The observed variations of energy may also be explained if the absorption in the shorter wave-lengths does not vary in phase with the total energy.

Irregular variables and other red stars.—Four M-type stars of this class were observed. Their variations in radiometric magnitude are small, probably about 1 mag. in five of the light-variation. Five N-type stars show the same characteristics. The lowest temperature so far measured for any star is somewhat less than 1500° K, for V Cygni near minimum. R Cygni, type Se, shows characteristics like those of Me stars. Ten faint stars of large color index were examined, but showed no characteristics which would place them in the class of the giant Me stars at minimum.

Cepheid variables.—The radiometric magnitudes of η Aquilae and δ Cephei are in phase with their light-curves. Unless the parallaxes are larger than those usually assigned, the variations in radial velocity are too small to be detected by radiation measurements involving errors greater than 0.01 mag.

Algol.—The radiometric changes in Algol are in phase with its variations in light. The measurements indicate that the eclipsing companion is of early type, but later than the primary component, as has been shown by the spectroscopic evidence. The range of brightness from beginning to middle eclipse is 1.08 mag. for both m_r and m_{WC}. The photoelectric range determined by Stebbins is 1.20 mag.

A brief statement of the observational data obtained on the radiation from variable stars at maximum and minimum phases has al-

[1] *Contributions from the Mount Wilson Observatory, Carnegie Institution of Washington*, No. 478.

ready been published.[2] The methods employed in making and reducing the observations have also been described.[3] The galvanometer deflections obtained with the vacuum thermocouple at the 100-inch telescope were reduced to a system of radiometric magnitudes and water-cell absorptions in which all instrumental and atmospheric variants were accounted for. The standard conditions selected were: star in the zenith at Mount Wilson; two reflections from fresh silver in the telescope; rock-salt window on the thermocouple. The radiometric system of magnitudes is so chosen that the radiometric and visual magnitudes are equal for the brighter stars of class Ao.

VARIABLE STARS OF LONG PERIOD

Nineteen stars of type Me and two of type Se were observed, six at all phases, five at most phases, and ten on only a few nights. The mean results from the eleven stars best observed were: radiometric range, 0.9 mag., corresponding to a visual range of 5.3 mag.; average temperature at maximum and minimum, 2350° and 1830° K; average diameter at maximum and minimum, 0″.025 and 0″.029; mean absolute bolometric magnitude, −3.2, corresponding to that of a Cepheid of about ten days' period. Detailed observations throughout the light-cycles of these stars will be discussed here.

Table I gives the observational data, including the visual magnitude m_v (obtained from the Harvard College Observatory), the radiometric magnitude m_r, and the water-cell absorption WC. The phase is determined from the light-curves independently for each cycle with the aid of the dates of the preceding and following maxima given in the second column. The visual magnitudes of *o* Ceti, X Ophiuchi, and R Aquarii in Table I have not been corrected for the light of the companion star, but such corrections have been included in the corresponding curves in Figures 1, 7, and 11.

The data in the last three columns of Table I (for the eleven stars best observed) are plotted against the phase from the third column in Figures 1–11 inclusive. The symbols employed show the cycle to which each observation belongs. Each plotted value of m_r and WC

[2] *Mt. Wilson Contr.*, No. 369; *Astrophysical Journal*, **68**, 279, 1928.

[3] *Ibid.*; *Mt. Wilson Contr.*, No. 246; *Astrophysical Journal*, **56**, 295, 1922.

TABLE I

OBSERVATIONS OF LONG-PERIOD VARIABLES

Julian Day		Vis. Phase	m_v	m_r	WC	Julian Day		Vis. Phase	m_v	m_r	WC
Obsn.	Max.*					Obsn.	Max.*				
					021403 o Ceti M6e						
242..	242..					242..	242..				
3233....	3172	0.20	5.3	−0.15	1.56	4051.....	.....	0.71	9.0	+0.80	1.97
3260.....	.....	.28	6.3	−0.05	1.67	4052.....	.....	.71	9.0	+ .76	1.94
3261.....	.....	.29	6.4	−0.06	1.66	4086.....	.....	.81	8.6	+ .65	1.78
3293.....	.....	.39	7.6	+0.26	1.81	4111.....	.....	.88	6.6	+ .39	.....
3295.....	.....	.40	7.7	+0.28	1.80	4139....	4153	.96	4.1	+ .01	1.29
3322.....	.....	.48	8.3	+0.50	1.96	4210.....	.....	.18	5.0	− .14	1.44
3380.....	.....	.67	8.3	+0.60	1.81	4358.....	.....	.60	8.8	+ .84	1.95
3381.....	.....	.67	8.2	+0.56	1.86	4380.....	.....	.67	9.1	+ .76	1.89
3411.....	.....	.77	7.9	+0.65	1.75	4407.....	.....	.75	8.4	+ .70	1.81
3472....	3482	.97	3.0	−0.04	1.22	4473....	4487	.96	3.6	− .11	1.31
3617.....	.....	.39	6.8	+0.33	1.92	4524.....	.....	.11	4.0	− .22	1.47
3645.....	.....	.47	8.2	+0.62	1.90	4564.....	.....	.23	5.6	− .22	1.60
3706.....	.....	.64	9.2	+1.01	2.18	4765.....	.....	.87	6.4	+ .46	1.64
3738.....	.....	.74	9.1	+1.16	2.13	4798....	4808	.97	3.4	− .15	1.12
3768.....	.....	.82	8.4	+0.98	1.77	4850.....	.....	.13	4.4	− .16	1.83
3795....	3830	.90	5.6	+0.43	1.51	4883.....	.....	0.23	5.4	−0.24	1.55
4027.....	.....	0.64	9.2	+0.85	2.06	.....	.....	.....	.....	.....	.....
					023133 R Trianguli M5e						
3322....	3346	0.91	7.3	3.75	1.50	4139....	4138	0.00	6.1	3.49	1.15
3382.....	.....	.14	7.6	3.38	1.30	4210.....	.....	.27	9.0	3.60	1.64
3412.....	.....	.25	8.9	3.62	1.23	4358.....	.....	.83	7.9	3.90	1.20
3472.....	.....	.48	11.4	4.36	1.65	4380.....	.....	.91	7.0	3.56	1.09
3473.....	.....	.48	11.5	4.25	.....	4407....	4404	.01	6.2	3.48	0.96
3645....	3610	.13	7.2	3.41	1.28	4408.....	.....	.02	6.3	3.58	0.64
3706.....	.....	.37	10.1	3.68	.....	4473.....	.....	.26	9.2	3.76	1.29
3768.....	.....	.60	11.2	4.07	1.65	4524.....	.....	.46	11.2	4.19	1.26
3795.....	.....	.71	9.5	3.99	1.34	4564....	4666	.62	10.4	4.23	1.18
3850....	3871	.92	6.9	3.81	1.22	4765.....	.....	0.36	10.5	4.17	1.34
4051....	.....	0.67	9.9	4.34	1.16	.....	.....	.....	.....	.....	.....
					081112 R Cancri M7e						
3173....	3135	0.10	8.1	1.71	1.73	3850....	3877	0.93	7.2	2.15	1.49
3174.....	.....	.10	8.2	2.16	1.46	3909.....	.....	.09	7.5	1.78	1.67
3324.....	.....	.51	11.3	2.86	2.72	4210....	4239	.92	8.2	2.50	1.43
3382.....	.....	.66	10.2	2.71	2.34	4270.....	.....	.08	7.9	2.14	1.81
3383.....	.....	.67	10.2	2.92	1.69	4473.....	.....	.63	10.9	2.68	2.00
3412.....	.....	.75	9.2	2.43	2.00	4524.....	.....	.77	10.0	2.64	1.82
3472....	3506	.91	8.1	2.43	1.51	4564.....	.....	.87	8.2	2.36	1.82
3738.....	.....	.62	10.2	2.48	2.41	4625....	4611	.04	7.0	1.82	1.94
3768.....	.....	.71	9.6	2.40	1.92	4850.....	.....	.64	11.2	3.12	2.30
3795.....	.....	0.78	9.2	2.37	1.81	4883....	4982	0.73	10.4	2.82	1.96

* Nearest visual max.

TABLE I—*Continued*

Julian Day		Vis. Phase	m_v	m_r	WC	Julian Day		Vis. Phase	m_v	m_r	WC
Obsn.	Max.*					Obsn.	Max.*				
				093934 R Leonis Minoris M8e							
242..	242..					242..	242..				
3382....	3120	0.72	11.8	2.80	2.17	4210....	4243	0.91	8.8	2.58	1.64
3412....	.....	.80	10.5	2.64	2.11	4268....	.....	.07	7.5	2.07	1.80
3472....	3485	.96	7.1	2.26	1.44	4296....	.....	.14	8.8	1.98	1.80
3557....	.....	.19	8.5	2.03	1.86	4525....	.....	.74	10.8	2.66	2.31
3740....	.....	.67	11.8	3.00	2.10	4564....	.....	.85	9.4	2.63	1.94
3768....	.....	.74	11.2	2.96	1.54	4592....	.....	.93	7.4	2.38	1.74
3795....	.....	.81	10.5	2.73	1.67	4624....	4620	.01	6.5	2.02	1.63
3850....	3866	.96	7.3	2.45	1.71	4671....	.....	.13	7.8	2.17	1.78
3908....	.....	.11	7.8	2.08	.....	4883....	.....	.69	12.3	3.04	1.94
3943....	.....	0.21	9.3	2.10	1.87	4997....	5002	0.99	7.1	2.12	1.52
				094211 R Leonis M8e							
3173....	3027	0.48	9.9	0.96	2.29	3908....	.....	0.83	8.4	0.60	2.04
3174....	.....	.48	9.9	1.11	2.24	3943....	3963	.94	6.2	.06	1.74
3196....	.....	.55	10.0	1.04	2.27	4210....	.....	.81	8.8	.83	1.99
3197....	.....	.55	10.0	1.00	2.30	4268....	4268	.00	6.2	.09	1.78
3325....	3334	.97	5.8	0.10	1.77	4296....	.....	.09	6.7	.11	1.91
3382....	.....	.16	6.6	0.15	1.94	4473....	.....	.69	9.3	.82	2.16
3384....	.....	.16	6.7	0.07	1.89	4524....	.....	.86	7.6	.55	1.85
3412....	.....	.26	7.8	0.22	2.09	4564....	4566	.99	5.8	.20	1.60
3472....	.....	.46	9.9	0.85	2.25	4592....	.....	.08	6.1	.30	1.53
3503....	.....	.56	10.2	0.97	2.10	4624....	.....	.19	6.8	.07	1.96
3533....	.....	.66	9.2	0.47	2.14	4655....	.....	.29	7.2	.44	2.13
3557....	3634	.74	8.4	0.53	1.99	4671....	.....	.34	7.9	.55	2.09
3739....	.....	.32	8.4	0.38	2.17	4850....	.....	.93	6.2	.37	1.59
3768....	.....	.41	9.3	0.72	2.31	4883....	4872	.04	5.9	.18	1.72
3795....	.....	.49	10.0	0.81	2.30	4997....	.....	0.41	8.5	0.24	2.18
3850....	.....	0.66	9.9	0.66	2.22	.....	.....	.....	.....	.....	.....
				132422 R Hydrae M8e							
3173....	3047	0.31	8.2	+0.25	2.06	3981....	.....	0.28	7.3	+0.00	2.00
3174....	.....	.31	8.2	+0.75	2.08	4210....	.....	.83	7.8	+ .48	1.66
3196....	.....	.36	8.8	+0.56	2.08	4268....	.....	.97	4.8	+ .06	1.54
3233....	.....	.46	9.5	+1.28	1.72	4296....	4282	.03	4.7	− .09	1.52
3260....	.....	.52	9.9	+1.00	2.05	4525....	.....	.58	9.4	+ .67	2.10
3413....	.....	.89	6.3	+0.48	1.56	4565....	.....	.68	8.5	+ .70	1.95
3472....	3455	.04	4.8	+0.06	1.50	4592....	.....	.74	7.7	+ .46	1.87
3503....	.....	.12	6.0	+0.02	1.72	4624....	.....	.82	7.2	+ .40	1.83
3557....	.....	.25	7.4	+0.07	1.95	4671....	.....	.93	5.3	+ .81	1.64
3796....	3863	.83	7.1	+0.37	1.66	4703....	4698	.01	4.6	+ .21	1.48
3908....	.....	.11	5.1	+0.18	1.65	4998....	.....	.73	7.7	+ .26	1.84
3943....	.....	0.19	6.2	−0.35	1.92	5045....	5109	0.84	6.0	+0.26	1.64

* Nearest visual max.

TABLE I—*Continued*

Julian Day		Vis. Phase	m_v	m_r	WC	Julian Day		Vis. Phase	m_v	m_r	WC
Obsn.	Max.*					Obsn.	Max.*				
183308 X Ophiuchi M6e											
242..	242..					242..	242..				
3196....	3155	0.12	7.1	1.64	1.81	4268....	.....	0.31	8.7	2.01	.....
3260....	.....	.31	8.4	1.84	1.99	4269....	.....	.32	8.7	1.94	2.01
3293....	.....	.41	8.7	2.11	.....	4296....	.....	.40	8.4	2.12	2.10
3322....	.....	.49	8.9	2.41	2.39	4358....	.....	.58	8.4	2.21	2.06
3533....	3493	.12	7.2	1.55	1.85	4380....	.....	.65	8.2	2.02	2.01
3557....	.....	.20	7.7	1.54	1.82	4381....	.....	.65	8.2	2.17	1.82
3620....	.....	.40	8.6	2.29	1.68	4446....	4498	.84	7.7	2.00	1.69
3644....	.....	.47	8.7	2.22	2.01	4593....	.....	.28	8.4	2.10	1.84
3908....	3814	.27	8.0	1.56	1.72	4654....	.....	.46	8.6	2.44	2.11
3943....	.....	.37	8.4	1.73	1.75	4703....	.....	.61	8.3	2.26	1.74
3944....	.....	.37	8.4	1.72	2.19	4734....	.....	.70	8.0	2.10	1.59
4027....	.....	.61	8.6	2.12	1.60	4768....	.....	.80	7.8	2.06	1.58
4051....	4163	.68	8.4	1.99	1.80	4798....	4836	0.89	7.2	1.90	1.31
4211....	.....	0.14	7.3	1.57	1.77	.....	.....	.....	.....	.....	.....
190108 R Aquilae M7e											
3196....	.....	0.84	9.8	2.89	1.95	4027....	.....	0.52	11.8	2.69	2.08
3233....	3246	.96	6.8	2.17	1.46	4051....	.....	.60	11.7	2.76	1.97
3260....	.....	.04	7.1	2.02	1.65	4268....	4174	.30	8.6	1.89	.....
3261....	.....	.05	7.2	1.98	1.66	4296....	.....	.40	9.6	2.04	1.92
3293....	.....	.15	8.4	2.03	1.91	4358....	.....	.60	10.9	2.66	2.21
3322....	.....	.24	9.8	2.15	2.14	4380....	.....	.67	10.6	2.24	2.01
3381....	.....	.44	11.1	2.83	.....	4407....	.....	.75	9.7	2.23	1.89
3382....	.....	.44	11.2	2.67	2.06	4446....	.....	.88	7.4	1.99	1.80
3534....	.....	.93	6.2	1.87	1.57	4474....	4483	.97	5.9	1.63	1.50
3558....	3556	.00	5.8	1.72	1.46	4624....	.....	.45	10.6	2.46	.....
3617....	.....	.19	7.9	1.79	1.78	4654....	.....	.55	11.5	2.81	1.92
3644....	.....	.28	8.8	2.04	1.95	4671....	.....	.60	11.2	2.80	2.11
3909....	3870	.13	7.6	1.65	1.87	4703....	.....	.70	10.4	2.58	1.83
3943....	.....	.24	9.8	1.95	2.08	4765....	.....	.90	7.2	2.18	1.40
3944....	.....	.24	10.0	1.90	1.91	4766....	.....	.90	7.0	2.11	1.50
3973....	.....	.34	10.7	2.09	2.26	4798....	4796	.01	6.0	1.71	1.46
3990....	.....	0.40	11.1	2.30	2.03	4998....	5097	0.67	10.7	2.10	1.96
193449 R Cygni Se											
3557....	.....	0.92	7.4	4.00	1.36	4381....	.....	0.82	10.1	4.26	1.44
3617....	3588	.07	6.5	3.76	1.07	4408....	.....	.88	9.1	4.20	1.52
3645....	.....	.13	7.6	3.55	1.49	4473....	4457	.04	7.1	3.54	1.20
4053....	4030	.05	8.4	3.80	1.11	4767....	.....	.72	13.6	5.02	.....
4086....	.....	.13	9.1	3.62	1.59	4799....	4889	0.79	12.1	4.38	1.66
4359....	.....	0.77	11.4	4.60	1.76	.....	.....	.....	.....	.....	.....

* Nearest visual max.

TABLE I—*Continued*

Julian Day		Vis. Phase	m_v	m_r	WC	Julian Day		Vis. Phase	m_v	m_r	WC
Obsn.	Max.*					Obsn.	Max.*				
					194632 χ Cygni M6pe						
242..	242..					242..	242..				
3233....	.....	0.77	9.9	1.18	1.81	4269....	.....	0.32	10.2	0.54	2.20
3293....	.....	.92	5.9	0.91	1.58	4296....	.....	.39	11.1	0.89	2.32
3295....	.....	.92	5.8	0.91	1.57	4358....	.....	.54	12.7	1.34	2.22
3322....	3326	.99	4.7	0.59	1.64	4380....	.....	.59	12.8	1.40	2.78
3382....	.....	.14	6.5	0.44	1.83	4407....	.....	.66	12.3	1.27	2.29
3533....	.....	.51	12.7	1.22	2.81	4408....	.....	.66	12.2	1.23	2.12
3617....	.....	.72	10.7	1.08	1.88	4473....	.....	.82	7.0	0.88	1.64
3644....	.....	.79	8.4	0.94	1.77	4593....	4549	.11	5.4	0.42	1.84
3738....	3730	.02	4.9	0.46	1.58	4624....	.....	.19	6.6	0.54	1.97
3908....	.....	.44	11.7	1.02	2.38	4654....	.....	.26	8.5	0.86	2.22
3909....	.....	.44	11.8	0.96	2.58	4671....	.....	.30	9.5	0.98	2.34
3944....	.....	.53	12.9	1.32	2.78	4703....	.....	.38	11.2	1.22	2.80
3974....	.....	.60	13.6	1.56	.....	4765....	.....	.54	12.7	1.71	2.43
3991....	.....	.64	13.4	1.76	.....	4766....	.....	.54	12.8	1.84	2.68
4027....	.....	.73	11.7	1.34	2.10	4799....	.....	.62	13.2	1.71	2.78
4051....	.....	.79	10.8	1.27	2.09	4997....	4952	.11	6.9	0.42	1.93
4086....	4136	.88	9.1	1.28	1.96	5067....	.....	0.28	9.7	0.49	2.32
4211....	.....	0.18	7.8	0.40	1.95	.....	.....	.....	.....	.....	.....
					233815 R Aquarii M7e (+Pec.)						
3293....	3072	0.57	9.7	2.52	2.31	3991....	.....	0.39	9.5	1.99	1.78
3295....	.....	.58	9.7	2.54	2.26	4053....	.....	.54	10.5	2.45	2.55
3322....	.....	.65	9.3	2.38	2.25	4086....	.....	.63	10.4	2.38	2.38
3381....	.....	.80	9.3	2.38	1.86	4111....	4230	.69	10.2	2.31	2.74
3411....	.....	.88	9.0	2.16	.....	4358....	.....	.33	9.6	2.08	2.20
3413....	3458	.88	8.9	2.04	1.92	4380....	.....	.38	9.7	2.11	2.23
3617....	.....	.42	9.3	2.27	1.84	4407....	.....	.45	10.1	2.46	2.22
3644....	.....	.49	9.4	2.27	2.07	4473....	.....	.62	9.9	2.74	2.76
3738....	.....	.73	9.1	2.14	2.44	4765....	4622	.37	9.9	2.12	1.98
3768....	3841	0.81	8.9	2.04	1.98	4798....	5008	0.46	9.8	2.22	2.08

* Nearest visual max.

represents a single observation, but the plotted m_v is the mean of several observations.

In the case of *o* Ceti, X Ophiuchi, and R Aquarii, the dotted portion of the light-curve shows the probable magnitude of the variable at minimum phase as determined from the relation between *HI* and *WC* already given,[4] thereby correcting the light-curve for the com-

[4] *Mt. Wilson Contr.*, No. 369; *Astrophysical Journal*, **68**, 279, Fig. 3, 1928.

panion star. In the case of *o* Ceti, the heat index at maximum light, which is not affected by the companion star, is 3.67 mag., 1.1 mag. greater than normal for its water-cell absorption. At minimum its

TABLE I*a*

Harv. No.	Name	Julian Day	Type	Vis. Phase	m_v	m_r	*WC*
		242..					
001755	T Cas	3324	M8e	0.21	9.4	1.7	2.3
084803	S Hya	3383	M4e	.84	8.8	5.5	>2.0
		3795	.....	.44	12.7	5.2	>2.5
		4524	.....	.27	11.9	4.7	>1.5
115919	R Com	4270	M4e	.91	10.2	6.5	>2.0
132706	S Vir	4269	M7e	.98	6.8	2.6	1.6
		4592	.....	.85	9.4	3.5	.....
		4625	.....	.94	7.6	3.2	1.8
134440	R C Vn	4269	M6e	.42	10.5	3.4	2.0
		4296	.....	.51	10.9	3.8	1.5
142205	RS Vir	4297	M6e	.28	.....	3.7	1.3
		4360	.....	.44	.....	4.2	>2.0
		4592	.....	.98	.....	3.6	.....
151714	S Ser	4297	M5e	.71	12.6	4.4	>2.0
		4360	.....	.88	11.7	4.7	>2.0
171401	Z Oph	3295	M2e	.65	12.3	7.5	.....
191017	T Sgr	3557	Se	.94	10.2	4.7	1.4
		3620	.....	.09	8.6	4.1	2.7
		3645	.....	.16	9.5	4.0	1.8
		4360	.....	.98	7.8	4.0	1.7
		4381	.....	.04	8.0	3.8	1.8
		4407	.....	.10	8.5	4.3	1.8
		4767	.....	.98	9.0	4.8	1.4
		4799	.....	.07	9.5	4.3	1.3
194048	RT Cyg	3261	M3e	.93	7.1	5.3	1.0
		3295	.....	.11	7.4	5.4	1.3
		3324	.....	0.26	8.7	5.4	1.9

water-cell absorption is 2.04 mag., corresponding to a normal heat index of 8.0 mag. On applying the correction +1.1 mag. found at maximum, the heat index becomes 9.1 mag., which, added to the radiometric magnitude at minimum, +0.86 mag., gives the visual magnitude at minimum, namely, 10.0. Combining this with the

visual magnitude of the binary at minimum, 9.0, we then obtain 9.6 for the visual magnitude of the companion star. Its value has been estimated[5] at 9.8.

The observational data for X Ophiuchi and R Aquarii are so scattered and deficient near maximum phase that estimates of the visual magnitude of the variable and its companion from the radiometric measurements are subject to much uncertainty. So little is known of these stars that the results, although somewhat uncertain, may be of interest.

For X Ophiuchi the heat index at maximum light, 4.76 mag., is 0.9 mag. greater than normal for its water-cell absorption, which gives for minimum light a heat index of 9.2 mag. Since m_r at this phase is 2.33, we find the visual magnitude of the variable at minimum to be 11.5—a value about a magnitude fainter than that estimated by G. Van Biesbroeck.[6] Since the observed m_v for the combined light of the two stars is 8.8 mag., the magnitude of the K-type companion would be 8.9.

R Aquarii is known as a double star only by its spectrum.[7] Its maximum light is about 6.5 mag.[8] The observed range in light, 3.5 mag., is much too small for its range in radiometric magnitude, 0.8 mag., or in its water-cell absorption, 1.0 mag., which is further evidence of a companion. The heat index at maximum, 4.6 mag., is normal for its water-cell absorption, 1.5 mag. The heat index at minimum corresponding to its water-cell absorption, 2.5 mag., is 11.2 mag. Adding the radiometric magnitude, 2.5, we find the visual magnitude at minimum to be 13.7, a range of 7 mag., which is normal for the range of 1 mag. in *WC*. The resulting magnitude of the companion star is 10.0.

An interesting fact shown by the curves in Figures 1–11 is that the radiometric magnitude is brightest about 0.1 cycle (30–40 days) after maximum visual brightness, and that the water-cell absorption is least at maximum visual brightness. Further evidence of the generality of this condition is given in Figure 12, which shows the aver-

[5] A. H. Joy, *Mt. Wilson Contr.*, No. 311; *Astrophysical Journal*, **63**, 281, 1926.

[6] *Publications of the Yerkes Observatory*, **5**, Part I, 136, 1927.

[7] P. W. Merrill, *Publications of the Astronomical Society of the Pacific*, **39**, 48, 1927.

[8] P. M. Ryves, *Monthly Notices of the Royal Astronomical Society*, **87**, 576, 1927.

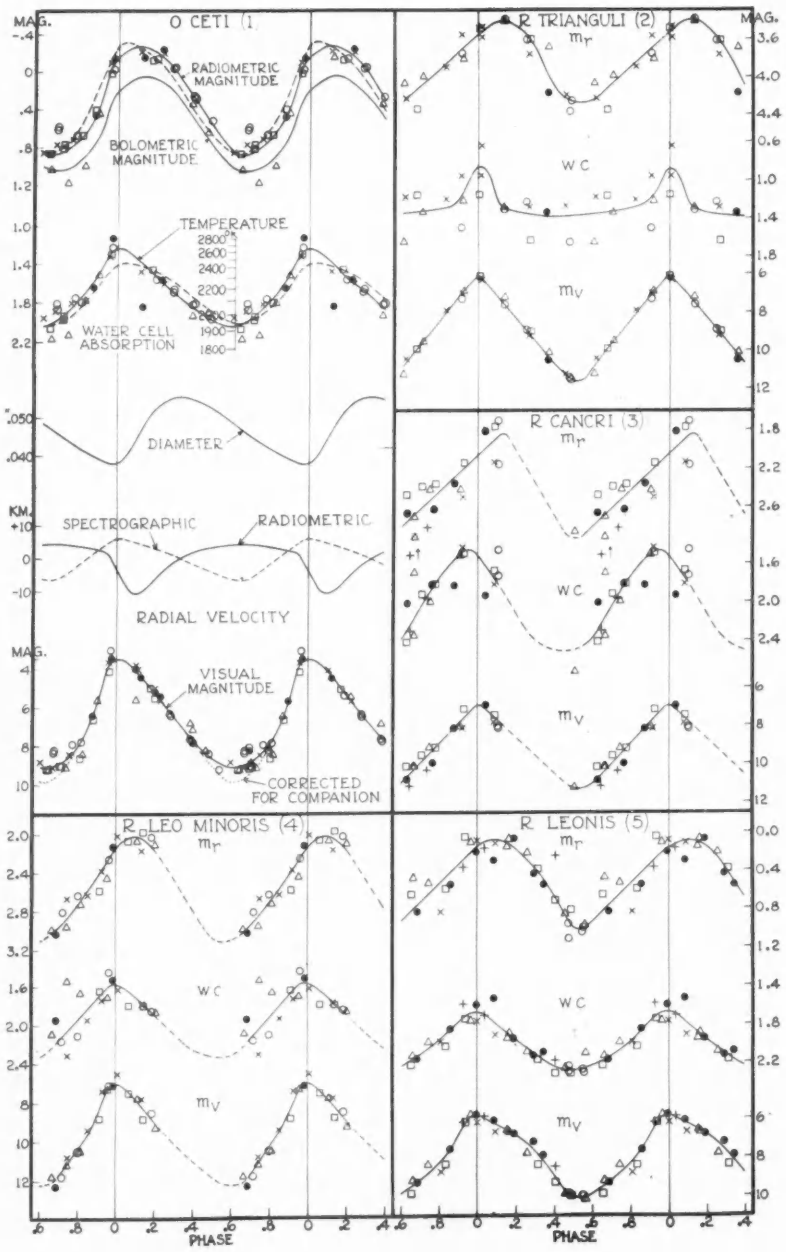

FIGS. 1–5.—Radiation-curves of long-period variable stars

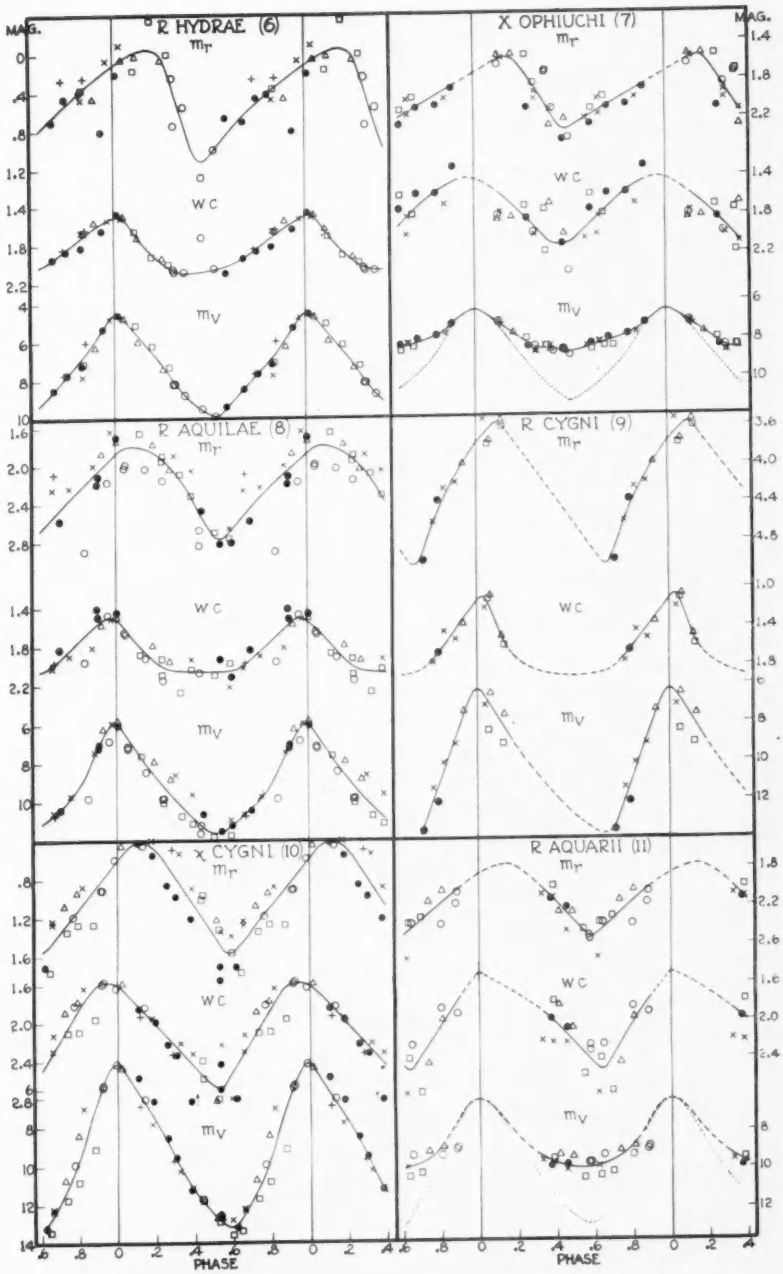

FIGS. 6–11.—Radiation-curves of long-period variable stars

age curves for the six best-determined stars, o Ceti, R Leonis Minoris, R Leonis, R Hydrae, R Aquilae, and χ Cygni, the average period of which is 359 days. The other stars lack observational data at critical points and have not been included in these averages. Interesting comparisons may also be made with the radiation transmitted by the water cell and with that eliminated by the water cell.

Magnitudes determined with the light transmitted by the water cell, m_{WC}, which includes most of the radiation from λ 0.3 to 1.3 μ, give a light-curve relating to the visual and near infra-red region. These magnitudes may be obtained by referring the deflections taken with the water cell in the light-path directly to the comparison stars, or from the relation

$$m_{WC}=m_r+WC\ , \tag{1}$$

where m_r is the radiometric magnitude and WC the water-cell absorption. Similarly, we may obtain magnitudes relating to the radiation of wave-length longer than 1.3 μ, which is not transmitted by the cell, from the relation,

$$m_W=m_{WC}-\frac{10}{4}\log\,(2.51^{(WC-0.08)}-1)-0.08\ , \tag{2}$$

where the constant, 0.08 mag., is due to the radiation reflected from the water cell. For the Me stars at minimum, the effect of this correction is +0.01 mag., but it becomes of greater importance for earlier classes, reaching +0.51 mag. for class Bo.

The bolometric magnitude m_b is given by the formula[9]

$$m_b=m_r-\Delta m_r+0.9\ , \tag{3}$$

where Δm_r is the reduction to no atmosphere, and the constant is so determined that $m_b=m_v$ for giant stars of type Go.

The mean curves for m_v, m_r, WC, m_{WC}, m_W, and m_b shown in Figure 12 are drawn to scales adjusted to give the curves approximately the same amplitudes, which facilitates the comparison of their shapes.

[9] *Mt. Wilson Contr.*, No. 369; *Astrophysical Journal*, **68**, 279, 1928. See the section entitled "Bolometric Magnitudes."

It will be noted that the maximum intensity of m_{WC} occurs 0.04 phase later than that of m_v; m_r, 0.1 phase later than m_v; and m_W and m_b, 0.14 phase later than m_v. Hence the maximum of emitted energy occurs later when we measure radiation of longer wave-lengths, where presumably the titanium oxide bands become less important. It appears, therefore, that the real maximum of energy in these stars is reached about phase 0.14, or 50 days, after the maximum of visual

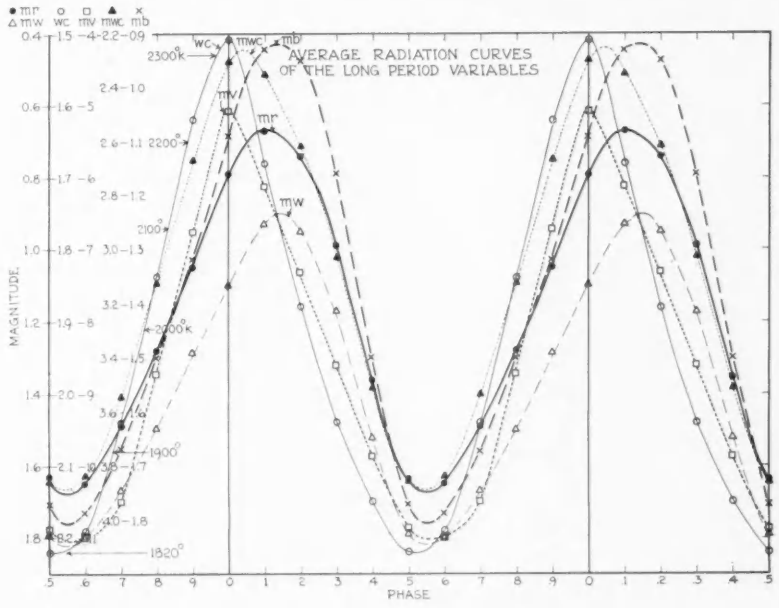

FIG. 12.—Average radiation-curves of the six best-determined long-period variable stars.

brightness, at a time when the stars are 1.5 mag. fainter than at maximum light.

The temperature indicated by the water-cell absorption reaches a maximum nearly at the time of maximum of light, but decreases relatively faster as minimum is approached. This circumstance probably accounts for the fact that the titanium oxide bands are weakest at maximum light and not at maximum energy. When the light is decreasing, the temperatures are lower than for the same magnitudes during increasing light. The maximum difference of about 150° C

occurs when the brightness is 2 or 3 mags. less than maximum light. To account for the observed phenomena by absorption alone would require a variation in the absorption of the star's atmosphere to the violet of 1.3 μ, which is not in phase with the variation of light. Changes in the star's diameter can be assumed which would bring the observations into accord, but those required do not agree with the velocity-curve in the case of o Ceti (Fig. 1), the only variable of this type for which a velocity-curve has been observed spectrographically.[5]

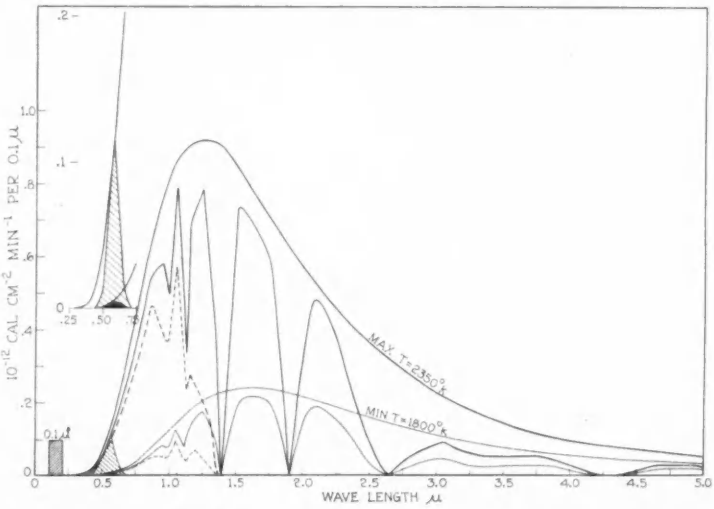

FIG. 13.—Spectral energy-curves of long-period variable stars at maximum and minimum of temperature and light.

Figure 13 shows the effects of the atmosphere and water cell on radiation from these stars considered as black bodies, near maximum and minimum temperatures. Black-body curves for 1800° and 2350° K have been multiplied by the transmission of the mean atmospheric water-vapor content[10] for Mount Wilson, 0.7 cm, and by the coefficients of reflection for two freshly silvered surfaces. The result is the energy as it would be observed at the telescope. The dotted curves show the radiation after transmission by the water

[10] *Mt. Wilson Contr.*, No. 369; *Astrophysical Journal*, **68**, 279, 1928.

cell. The intensity scale corresponds to zero radiometric magnitude, which is the average of the six best-observed stars at maximum outside our atmosphere.

The visual sensibility-curve (maximum at λ 0.555 μ), multiplied by the energy from the curve inside the atmosphere, is shown on an enlarged scale above its position on the principal curve. It will be noted that the energy concerned in the large variations of visual magnitude is but a small fraction of the total, whereas that concerned with the smaller variation of the whole radiation is large. The data in Table II were obtained from curves of this sort connecting temperature with water-cell absorption and heat index. A measurement of the areas of these curves gives the following results: (1) the water-cell absorption, which is practically confined to the violet slope of the energy-curve, varies from 1.5 at maximum to 2.3 mag. at minimum. The actual observed averages from Figure 12 are 1.5 and 2.2 mag., respectively. Since the temperatures were determined from the water-cell absorptions, the agreement ought to be exact, the small difference of 0.1 mag. being due to the use of 1800° K in making the curve instead of the observed mean, 1830° K. (2) The range in light between maximum and minimum temperatures is 3.4 mag., while the actual observed range shown in Figure 12 is 6 mag. The former range depends on an assumed constant stellar diameter and will be affected by any changes in this dimension between maximum and minimum, as will be discussed later. At least a part of this discrepancy of 2.6 mag. must be due to absorption in the atmosphere of the star, which affects the visual light much more than the near infra-red.[5] Titanium oxide is probably the principal absorbent.

The heat index is not, therefore, a simple criterion of temperature, and the water-cell absorption probably gives a much nearer approximation. Even the water-cell absorption is to some extent affected by titanium oxide, since, as A. S. King[11] has shown, these bands are present at wave-lengths approaching 1 μ, but, being less frequent there than in the visual region, do not affect the water-cell absorptions as much as the heat indices. We have therefore estimated the temperatures from water-cell absorptions only.

[11] Unpublished observations.

TEMPERATURES AND DIAMETERS FROM RADIATION MEASUREMENTS

We have already given in tabular form[12] the temperature of a star as a function of its water-cell absorption and also of its heat index, obtained on the assumption of black-body radiation passing through an atmosphere with a water-vapor content of 0.7 cm as above Mount Wilson, two reflections from silver, and a rock-salt

TABLE II

COMPUTED HEAT INDEX AND WATER-CELL ABSORPTION

Absolute Centigrade Temperature	Heat Index		Water-Cell Absorption	Atmospheric Absorption Δm_r
	λ 0.555 μ	λ 0.529 μ		
	Mag.	Mag.	Mag.	Mag.
24000°	+0.01	+0.01	+0.17	+2.84
20000	0.01	0.01	0.18	2.35
16000	0.01	0.00	0.19	1.84
14000	0.00	0.00	0.20	1.57
12000	0.00	0.00	0.21	1.26
10000	0.02	0.05	0.24	1.00
8000	0.07	0.12	0.29	0.71
7000	0.12	0.18	0.32	0.60
6000	0.26	0.33	0.37	0.49
5000	0.48	0.59	0.46	0.41
4000	0.92	1.08	0.63	0.41
3000	1.91	2.24	1.00	0.48
2500	2.81	3.32	1.34	0.57
2000	4.33	5.16	1.93	0.71
1500	+7.29	+8.58	+3.03	+0.96

window on the thermocouple. For convenience, the results are reprinted in Table II. Between 5000° and 1500° K, these temperatures are represented by the simple relationship

$$T = 3000^\circ\ WC^{-\frac{1}{3}} \qquad (3.03 > WC > 0.46)\ , \tag{4}$$

with maximum errors of +66° at 1500° K and −50° at 4000° K. For temperatures greater than 6000° K the equation does not give even approximate values of T. Below 4000° K the exponent −0.623 gives

[12] *Mt. Wilson Contr.*, No. 369; *Astrophysical Journal*, **68**, 279, 1928, Table IV.

better values of T, the maximum deviation being $-9°$ at 2000° K. A modified form of the equation, namely,

$$\log T = 3.477 - 0.623 \log WC \qquad (3.03 > WC > 0.63)\,, \tag{5}$$

is more convenient for computation.

If a star radiates like a black body without darkening at the limb, its diameter, d, is given by

$$\log d = 5.276 - 2 \log T - 0.2\,(m_r - \Delta m_r)\,, \tag{6}$$

where Δm_r, the atmospheric absorption in magnitudes, is connected with the water-cell absorption, WC, by the linear relation

$$\Delta m_r = 0.252 + 0.234 WC \qquad (3.03 > WC > 0.63)\,, \tag{7}$$

for which the maximum error is 0.01 mag. at $WC = 0.63$. Substituting the equivalents of $\log T$ and Δm_r from equations (5) and (7) into (6), we obtain

$$\log d = 1.246 \log WC + 0.0468\, WC - 0.2 m_r - 1.628 \tag{8}$$

$$(3.03 > WC > 0.63)\,.$$

Equations (5), (7), and (8) hold only for stars later than gG6 and dK2. The temperatures and diameters given in Table III were computed with formulae (5) and (8).

The average diameters of the six best-observed long-period variables in this table are 18 per cent larger at minimum than at maximum light. The theoretical range of 3.4 mag. in visual light was based on the WC temperature and on the assumption of constant diameter. If the variation in diameter is real, the computed visual range would be 3.1 mag., leaving a discrepancy of 2.9 instead of 2.6 mag. between the observed range and that computed from black-body conditions.

The effect of darkening at the limb on the computed diameters and temperatures of stars is known only for the sun. Eclipsing variables indicate that darkening at the limb exists, but give little evidence as to the amount. Just what should be expected in the long-period variables is difficult to surmise, but probably we should come

nearer the truth by applying corrections for darkening in total radiation as though the star behaved like our sun.[13]

TABLE III

TEMPERATURES AND DIAMETERS OF THE LONG-PERIOD VARIABLES

Visual Phase	m_r	WC	T	d	Visual Phase	m_r	WC	T	d
	021403 o Ceti M6e					023133 R Trianguli M5e			
0.0	−0.19	1.23	2640°	0″.038	0.0	3.54	0.87	3270°	0″.0043
.1	− .28	1.34	2500	.044	.1	3.41	1.19	2690	.0069
.2	− .21	1.53	2300	.052	.2	3.48	1.33	2510	.0078
.3	− .01	1.70	2160	.055	.3	3.71	1.37	2470	.0073
.4	+ .31	1.87	2030	.055	.4	4.11	1.38	2460	.0062
.5	+ .58	1.98	1960	.052	.5	4.26	1.37	2470	.0056
.6	+ .83	2.04	1920	.049	.6	4.24	1.35	2490	.0056
.7	+ .83	1.94	1990	.045	.7	4.08	1.33	2510	.0059
.8	+ .68	1.75	2120	.042	.8	3.89	1.30	2550	.0063
0.9	+0.33	1.49	2340	0.039	0.9	3.72	1.19	2690	0.0060
	081112 R Cancri M7e					093934 R Leonis Minoris M8e			
0.0	2.06	1.52	2310°	0″.018	0.0	2.14	1.57	2270°	0″.018
.1	1.88	1.80	2080	.025	.1	2.02	1.71	2150	.022
.2	(2.03)	(2.12)	(1880)	(.030)	.2	2.16	1.89	2020	.024
.3	(2.37)	(2.40)	(1740)	(.031)	.3	(2.47)	(2.09)	(1900)	(.024)
.4	(2.70)	(2.49)	(1700)	(.028)	.4	(2.78)	(2.25)	(1810)	(.023)
.5	2.94	2.49	1700	.025	.5	(3.08)	(2.32)	(1780)	(.021)
.6	2.81	2.38	1750	.025	.6	(3.11)	(2.32)	(1780)	(.021)
.7	2.62	2.04	1920	.021	.7	2.95	2.15	1860	.020
.8	2.44	1.73	2130	.018	.8	2.71	1.91	2000	.019
0.9	2.25	1.51	2320	0.016	0.9	2.44	1.71	2150	0.018
	094211 R Leonis M8e					*132422* R Hydrae M8e			
0.0	0.17	1.68	2170°	0″.050	0.0	+0.12	1.50	2330°	0″.043
.1	0.10	1.80	2080	.057	.1	−0.01	1.65	2190	.053
.2	0.17	1.97	1970	.062	.2	−0.04	1.89	2020	.065
.3	0.38	2.11	1880	.063	.3	+0.30	2.05	1920	.062
.4	0.68	2.24	1820	.060	.4	+0.95	2.08	1900	.047
.5	1.00	2.28	1800	.053	.5	+1.06	2.06	1910	.044
.6	0.93	2.23	1820	.053	.6	+0.81	2.02	1940	.048
.7	0.74	2.13	1880	.054	.7	+0.61	1.91	2010	.049
.8	0.55	1.98	1960	.053	.8	+0.43	1.76	2110	.047
0.9	0.35	1.78	2090	0.050	0.9	+0.27	1.61	2230	0.045

[13] E. A. Milne, *Philosophical Transactions of the Royal Society*, A, **223**, 208, 1923; *Handbuch der Astrophysik*, **3**, Erste Hälfte, **148**, 1930.

TABLE III—*Continued*

Visual Phase	m_r	*WC*	*T*	*d*	Visual Phase	m_r	*WC*	*T*	*d*
183308 X Ophiuchi M6e					190108 R Aquilae M7e				
0.0	1.74	1.44	2390°	0″.019	0.0	1.87	1.51	2320°	0″.020
.1	1.62	1.54	2290	.023	.1	1.79	1.72	2140	.024
.2	1.58	1.70	2160	.026	.2	1.87	1.93	1990	.028
.3	1.84	1.89	2020	.027	.3	2.04	2.04	1920	.028
.4	2.16	2.10	1890	.028	.4	2.34	2.04	1920	.024
.5	2.32	2.10	1890	.026	.5	2.70	2.05	1920	.021
.6	2.20	1.93	1990	.024	.6	2.68	2.04	1920	.021
.7	2.08	1.73	2130	.022	.7	2.45	1.93	1990	.021
.8	1.97	1.56	2280	.020	.8	2.24	1.75	2120	.020
0.9	1.85	1.46	2370	0.019	0.9	2.06	1.56	2280	0.019
193449 R Cygni Se					194632 χ Cygni M6pe				
0.0	3.78	1.12	2790°	0″.0054	0.0	0.60	1.60	2240°	0″.038
.1	3.58	1.38	2460	.0078	.1	0.42	1.80	2080	.049
.2	(3.80)	(1.72)	(2140)	(.0097)	.2	0.49	2.03	1930	.057
.3	(4.06)	(1.85)	(2050)	(.0095)	.3	0.77	2.24	1820	.057
.4	(4.32)	(1.90)	(2010)	(.0088)	.4	1.08	2.45	1720	.057
.5	(4.59)	(1.90)	(2010)	(.0078)	.5	1.39	2.64	1640	.056
.6	(4.86)	(1.90)	(2010)	(.0069)	.6	1.56	2.50	1700	.047
.7	(4.97)	(1.84)	(2050)	(.0062)	.7	1.34	2.16	1860	.042
.8	4.44	1.64	2200	.0067	.8	1.09	1.84	2050	.037
0.9	4.08	1.38	2460	0.0062	0.9	0.85	1.60	2240	0.034
233815 R Aquarii M7e (+Pec.)					R Aquarii (*cont.*)				
0.0	(1.87)	(1.50)	(2330°)	(0″.019)	0.5	2.38	2.24	1820°	0″.027
.1	(1.79)	(1.60)	(2240)	(.022)	.6	2.51	2.46	1710	.030
.2	(1.81)	(1.72)	(2140)	(.024)	.7	2.33	2.34	1770	.030
.3	(1.96)	(1.86)	(2040)	(.025)	.8	2.16	2.02	1940	.026
0.4	2.16	2.03	1930	0.026	0.9	2.00	1.74	2120	0.023

We have already pointed out that the total radiation per unit area from the center of the sun is 16 per cent greater than the average from the disk;[14] hence a solar constant of 2.25 cal cm^{-2} min^{-1} should be used in computing the solar temperature from Stefan's law. The result thus found, 5960° K, was based on a series of drift-curves made in the laboratory in Pasadena in July and August, 1921,

[14] *Mt. Wilson Contr.*, No. 397; *Astrophysical Journal*, **71**, 153, 1930.

with a vacuum thermocouple and 6-inch glass objective of 30-foot focal length. These measures were repeated in 1933 with a concave mirror of 40-foot focal length and a galvanometer circuit of 0.27 sec. period. Results for the intensities along a solar radius in units of the intensity at the center of the disk are given in Table IV.

TABLE IV

INTENSITIES OF TOTAL RADIATION ALONG A RADIUS OF THE SOLAR DISK

YEAR	r									
	0.0	0.2	0.4	0.5	0.6	0.7	0.8	0.85	0.9	0.95
1921.....	1.00	0.99	0.96	0.94	0.92	0.88	0.83	0.80	0.76	0.69
1933.....	1.00	0.98	0.96	0.94	0.91	0.88	0.84	0.79	0.74	0.68

The averages of these figures show that the ratio of the intensity at the center of the disk to that from the disk as a whole is 1.17. Since temperatures of stars computed from radiation data are effective temperatures for the whole disk, it follows that for darkening toward the limb like that of the sun they should be increased by 4 per cent to obtain the effective temperatures at the center of the disk, i.e., photospheric temperatures. The diameters computed by equation (8), on the other hand, will be subject to little error, because of the manner in which the values of WC and m_r enter into this equation.

VELOCITIES OF PULSATION

If the variation in diameter obtained from the radiation measures is real, we may compute the radial velocity from one-half the first derivative of the diameter-curve corrected for the average projection on the line of sight according to the formula

$$v = -\frac{3}{8}\frac{R\delta d}{\pi\,\delta t}, \tag{9}$$

where π is the parallax, R the astronomical unit, d the angular diameter, and v the radial velocity in the same units as R and t. Figure 1 shows the velocity-curve for o Ceti, obtained in this manner from the radiometric data and a parallax of $0''.017$, compared with that

obtained by Joy (dotted curve)[15] from the absorption lines in the spectrum of the star. Although the amplitudes of the variations in the computed and the spectroscopic radial velocities are of the same order of magnitude, they are nearly opposite in phase.

OBSERVATIONS OF ADDITIONAL VARIABLES OF TYPE Me

In addition to the eleven Me variables regularly observed, ten others were measured on a few nights in order to see whether any of them have abnormal water-cell absorptions or radiometric magnitudes. The observational data are given in Table I*a*. Since these stars are fainter than the eleven already discussed, the errors of measurement are larger; but there is no evidence that any of them is in any way abnormal. The conclusions drawn from the six best-observed stars are, therefore, probably characteristic of Me variables in general.

IRREGULAR VARIABLES AND OTHER RED STARS

Four irregular variables of type M and five stars of type N were also measured from time to time. The results are given in Table V. The ranges in the individual values of m_r and *WC* are small, and we may judge whether they represent real variations by comparing them with the residuals obtained from stars of known constancy. The average residual for m_r, without regard to sign, is 0.03 mag. for stars of 0.0 radiometric magnitude, and increases with increasing magnitude to 0.08 mag. for $m_r = 3.0$ and to 0.12 mag. for $m_r = 4.0$. The average residuals for three irregular M-type variables, Betelgeuse, α Herculis, and R Lyrae, are about 0.02 mag. larger than the mean for standard stars of the same brightness. Since the stars of constant magnitude were used as standards for determining the other magnitudes, they should give somewhat smaller residuals, and the evidence of variability is, therefore, very slight. The mean residual for ρ Persei just equals the mean for stars of the same radiometric magnitude, and therefore indicates no significant variation in its total energy.

The best evidence of variability among the N-type stars is that supplied by U Hydrae, the mean residual for which is 0.07 mag.

[15] *Op. cit.*

larger than for the standard stars of comparable radiometric magnitude.

TABLE V

Julian Day	m_r	WC
Betelgeuse M2		
242..		
3174	−1.61	1.25
3296	1.62	1.16
3472	1.64	1.19
3503	1.70	1.14
3796	1.84	1.15
4524	1.67	1.19
4525	1.58	1.23
4564	1.71	1.19
4884	−1.63	1.19
ρ Persei M4		
3324	0.67	1.43
3645	.64	1.25
3740	.63	1.23
4110	.68	1.32
4381	.63	1.31
4474	0.58	1.15
R Lyrae M5		
3197	0.62	1.43
3233	.68	1.36
3295	.67	1.38
3324	.59	1.58
3383	.62	1.44
3533	.56	1.45
3588	.63	1.80
3644	.70	1.41
3908	.49	1.46
4027	.62	1.34
4052	.50	1.40
4268	.64	1.50
4269	.57	1.28
4359	.59	1.49
4380	.56	1.48
4407	.65	1.40
4592	.64	1.38
4624	.65	1.42
4671	.82	1.49
4703	.76	1.57
4765	0.66	1.38

Julian Day	m_r	WC
α Herculis M5		
242..		
3173	−0.83	1.55
3196	.78	1.42
3197	.77	1.43
3233	.67	1.51
3260	.72	1.54
3261	.72	1.50
3295	.69	1.46
3323	.73	1.56
3533	.87	1.54
3588	.80	1.50
3646	.79	1.46
3944	.88	1.48
4296	.76	1.59
4624	−0.78	1.52
19 Piscium N0		
3295	2.02	1.52
3382	2.15	1.40
4359	2.03	1.49
4381	2.16	1.54
U Hydrae N2		
3173	2.10	1.48
3174	2.16	1.41
3413	2.23	1.48
3472	2.42	1.39
3769	2.26	1.46
3796	2.07	1.52
3909	2.07	1.80
4210	2.19	1.47
4270	2.47	1.57
4297	2.33	1.33
4525	2.17	1.59
4625	2.35	1.89
4998	2.39	1.00

TABLE V—*Continued*

Julian Day	m_r	*WC*
X Cancri N3		
242..		
3173	3.04	1.30
3174	3.29	1.65
3383	3.17	1.67
3412	3.37	1.66
3768	3.20	1.51
3909	3.14	1.62
4270	3.47	1.54
4524	3.03	1.66
4625	3.29	1.90
4850	3.28	1.50
VX Andromedae N7		
242..		
3233	4.37	2.44
3293	4.14	1.56
3324	4.07	1.34
3383	4.22	1.69
4053	4.33	1.61
4359	3.96	2.22
4408	4.25	2.07
V Cygni N		
4051	3.51	3.46
4408	3.69	3.52

Another test of the reality of variability is the correlation of the variation of radiometric magnitudes with the variation of water-cell absorptions. The correlation plots for these stars are in general too scattered to afford definite conclusions, but Betelgeuse and U Hydrae show a definite increase of about 0.7 mag. in water-cell absorption per magnitude increase in m_r, as in the case of the long-period variables, thus indicating that the observed changes in these stars are probably real.

The largest water-cell absorption observed for any star is 3.5 mag., for the N-type variable V Cygni. The phases for the two observations made on this star were 0.68 and 0.56, respectively; the visual magnitudes, 10.7 and 11.5; and the resulting heat indices, 7.2 and 7.8 mag. Me-type variables with equivalent heat indices would have water-cell absorptions of 1.9 and 2.0 mag. The computed water-cell absorptions for black bodies with these heat indices are 3.0 and 3.1. The observed water-cell absorption and heat index indicate a temperature below 1500° K. V Cygni agrees with other stars of N type in indicating that they radiate more like black bodies than do the M-type stars having the same water-cell absorption.

Only one star of type Se, R Cygni, was observed at enough phases to give an idea of its energy- and temperature-curves. The data for

this star are in Table I. The variations in energy and temperature (Fig. 9) are essentially like those of the Me stars. χ Cygni has some of the spectral characteristics of S-type stars, but its radiometric curves show no marked deviations from those of normal Me stars.

Ten faint stars of exceptionally large color index and of visual magnitude approximating that of the Me stars near minimum were observed on the recommendation of Merrill and M. L. Humason. None of these showed a sensible deflection, thus indicating heat indices not exceeding 4 mag. These stars are not, therefore, of the class of the giant Me stars at minimum.

CEPHEID VARIABLES

Two of the brightest Cepheid variables, η Aquilae and δ Cephei, have been observed throughout the series of measurements. The individual observations are given in Table VI. The epoch of observation is Greenwich Mean Time, which has been reduced to the sun in the customary manner. The phases for η Aquilae have been computed from the visual maxima given by[16]

$$\text{J.D.} = 2408827.690 + 7^{d}.1765164E + 0.288 \times 10^{-7}E^{2} ;$$

those for δ Cephei by

$$\text{J.D.} = 2393659.873 + 5^{d}.366396E - 0.84 \times 10^{-8}E^{2} .$$

The median radiometric magnitudes of these stars, 3.46 and 3.66, respectively, are so faint that their accuracy is considerably less than for the bright Me stars. The water-cell absorption, which depends on the combination of measurements of free and water-cell deflections, is more uncertain than the radiometric magnitude, which depends on the free deflection alone; and, since its absolute value is small for stars of this spectral class, the percentage error is much larger than for the Me stars. The curve of water-cell magnitude, which involves errors of the water-cell deflection only and has a much larger amplitude than the water-cell absorption, was easier to draw; hence, for these stars the radiometric and water-cell magnitudes were plotted

[16] *Kleinere Veröffentlichungen der Universitätssternwarte zu Berlin-Babelsberg*, No. 11, 1933.

and the water-cell absorption determined for different phases by forming the difference between the mean curves. The water-cell magnitude, water-cell absorption, and radiometric magnitude are all

TABLE VI

Julian Day	Visual Phase	m_r	m_{wc}	Julian Day	Visual Phase	m_r	m_{wc}
η Aquilae				δ Cephei			
242..				242..			
3233.885	0.392	3.45	3.97	3260.739	0.018	3.42	3.74
3293.739	.732	3.69	4.33	3261.750	.207	3.50	4.02
3295.755	.014	3.22	3.64	3261.933	.241	3.47	3.98
3322.733	.772	3.65	4.34	3295.669	.527	3.74	4.18
3323.738	.912	3.44	4.06	3324.656	.929	3.47	4.00
3382.611	.116	3.25	3.80	3324.794	.955	3.40	3.93
3620.794	.305	3.43	3.83	3644.697	.567	3.75	4.30
3644.744	.642	3.71	4.18	3645.683	.751	3.84	4.44
3645.721	.779	3.80	4.28	3646.896	.977	3.51	3.92
3646.787	.927	3.39	3.82	3739.782	.285	3.74	4.06
3908.993	.464	3.39	3.86	3768.703	.675	3.78	4.44
3909.965	.599	3.57	4.13	3795.629	.693	3.78	4.35
3910.927	.733	3.70	4.20	3796.627	.876	3.67	4.22
3943.954	.336	3.38	3.92	4051.933	.454	3.92	4.18
3990.785	.861	3.33	3.86	4052.970	.647	3.93	4.31
3991.945	.023	3.22	3.54	4053.958	.831	4.01	4.31
4027.658	.999	3.21	3.70	4139.701	.808	3.50	3.91
4051.668	.344	3.40	3.89	4359.777	.818	3.80	4.34
4053.669	.623	3.93	4.24	4360.727	.995	3.56	3.81
4269.985	.766	3.55	4.22	4381.760	.914	3.76	4.01
4296.962	524	3.58	4.29	4407.952	.795	3.69	4.46
4297.958	.663	3.63	4.29	4408.943	.980	3.46	3.71
4358.823	.145	3.28	3.92	4474.767	.246	3.76	4.15
4359.957	.303	3.42	3.77	4525.629	.728	4.08	4.57
4360.904	.435	3.53	4.25	4703.809	0.113	3.42	.....
4380.674	.190	3.24	3.81				
4381.732	.337	3.33	3.78				
4407.688	.953	3.30	3.83				
4408.647	.087	3.38	3.63				
4474.616	.280	3.24	3.90				
4671.947	.777	3.74	4.28				
4703.925	0.233	3.45	4.23				

sensibly in phase with the visual magnitude. This result was to be expected, since the maximum of energy for stars of this class is in the visual region of the spectrum.

For temperatures such as occur on the Cepheids, the change of water-cell absorption with temperature is so small that tempera-

tures and diameters computed from water-cell absorptions are subject to considerable uncertainty. The rate of change of the computed diameters is still more uncertain, and parallaxes determined from radial velocities obtained from these measures have practically no weight. The mean diameters for these stars computed from equation (6) are: η Aquilae, 0".0021; δ Cephei, 0".0017.

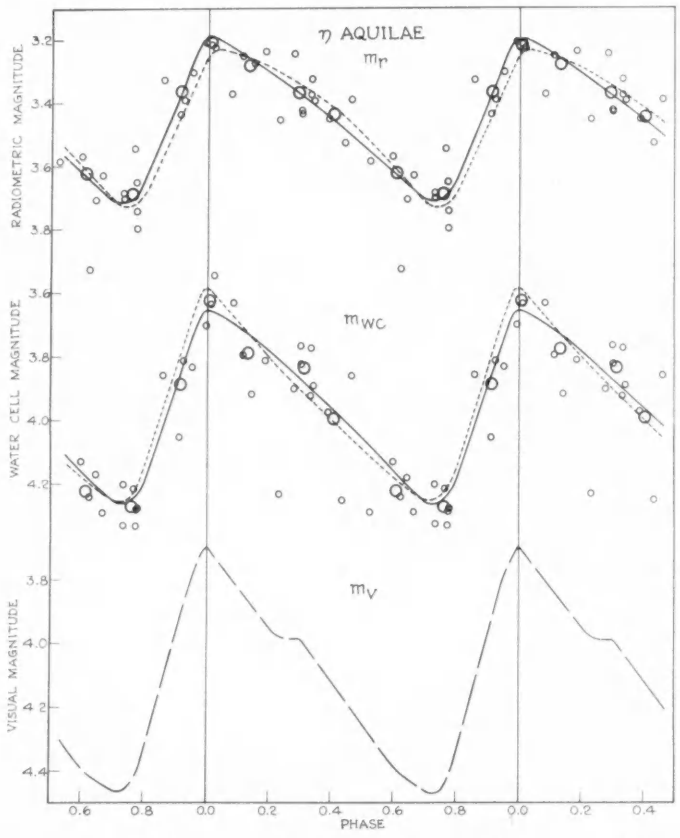

FIG. 14.—Radiation-curves of η Aquilae. Large circles are normal places

The full lines in Figures 14 and 15 conform to constant diameter. The dotted lines conform to the spectroscopic velocities interpreted as pulsations and to parallaxes four times those given by the period-luminosity law.[17] The curves corresponding to the parallaxes deter-

[17] H. Shapley, *Mt. Wilson Contr.*, No. 153, 145, 1918; *Astrophysical Journal*, **48**, 279, 1918.

mined from the period-luminosity law, values for which are given in Table VII, would lie one-fourth of the way from the full line to the dotted line, since constant diameter implies that the pulsations subtend a negligible angle. These two curves represent the observations about equally well; any study of diameters and parallaxes is therefore prevented.

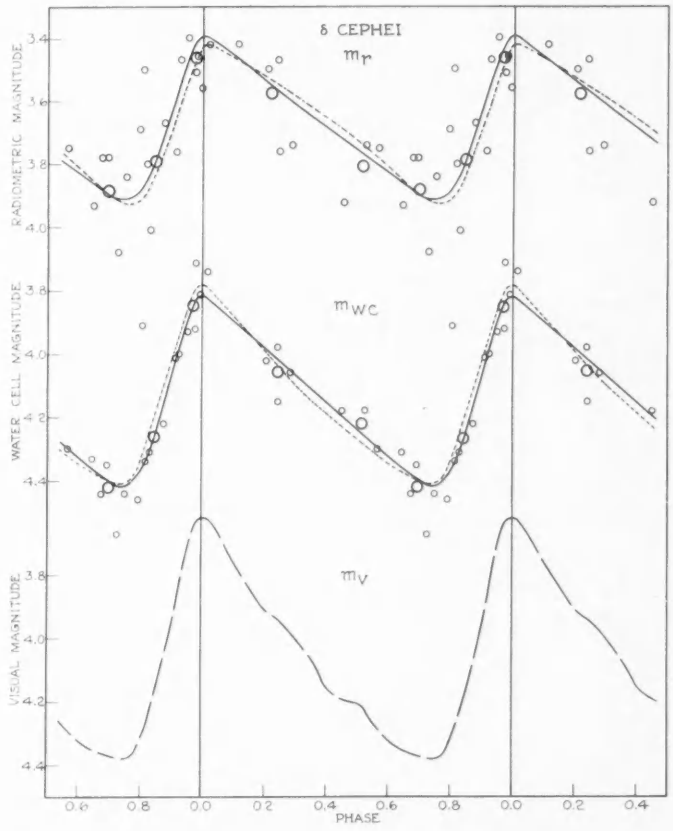

FIG. 15.—Radiation-curves of δ Cephei. Large circles are normal places

The visual magnitudes of η Aquilae were obtained from the average of the light-curves determined by F. Becker,[18] G. Hornig,[19] E. Breson,[20] and A. V. Nielsen.[21] These curves are from estimates by

[18] *Astronomische Nachrichten*, **225**, 1, 1925.

[19] *Ibid.*, **201**, 154, 1915.

[20] *Ibid.*, **196**, 139, 1913.

[21] *Ibid.*, **236**, 58, 1929.

the step method relative to a field of comparison stars. The mean curve from these data is the broken line in Figure 14.

For δ Cephei the measures giving the best determination of the light-curve are probably those of J. Stebbins,[22] who made comparisons with the optical companion by using a polarizing photometer. The range observed was greater than that of the other observers, but was not subject to correction for the light of the optical companion. The scale was fundamentally determined and does not depend on the magnitudes of different comparison stars. No scale zero was given, however, as the magnitude of the comparison star is somewhat uncertain. The zero point was determined for this paper by using the mean magnitude from the curves of S. P. Glasenapp and S. Beliawsky,[23] M. Luizet,[24] H. E. Lau,[25] E. Breson,[26] G. Hornig,[27] E. H. Vogelzang,[28] and A. Johansson and A. V. Nielsen,[29] corrected for the light of the companion, which obviously was included in all these estimates. The mean curve fits that given by Stebbins best when a value of 6.55 mag. is assigned to the companion of δ Cephei. The curve of Stebbins thus adjusted for zero point is shown by a broken line in Figure 15.

Table VII gives data for each tenth phase, and Table VIII a summary relating to maxima and minima, in which m_r, m_v, m_{pe}, m_{WC}, and m_b are the radiometric, visual, photoelectric, water-cell, and bolometric magnitudes, respectively.

The photoelectric measures are those of C. C. Wylie[30] and P. Guthnick,[31] who used potassium and rubidium cells, respectively, both of which are sensitive to an effective wave-length of about λ 0.46 μ. The zeros of the scales were obtained for this paper by adding 0.7 of the color index[32] to the visual magnitudes of the comparison

[22] *Astrophysical Journal*, **27**, 188, 1908.

[23] *Astronomische Nachrichten*, **165**, 225, 1904.

[24] *Annales de l'Université de Lyon: Nouvelle série*, Fasc. 33, 1912.

[25] *Astronomische Nachrichten*, **194**, 231, 1912.

[26] *Ibid.*, **196**, 139, 1913.

[27] *Ibid.*, **201**, 154, 1915.

[28] *Ibid.*, **214**, 265, 1921.

[29] *Ibid.*, **227**, 139, 1926.

[30] *Astrophysical Journal*, **56**, 217, 1922.

[31] *Astronomische Nachrichten*, **208**, 169, 1919.

[32] J. Stebbins, *Publications of the Washburn Observatory*, **15**, Pt. 1, 1928.

stars, making the photoelectric magnitude of β Aquilae, 4.60, and of ϵ Cephei, 4.43. The bolometric magnitude was obtained from equation (3). In Table VIII, *WC* is the water-cell absorption obtained from the water-cell magnitude by equation (1). The heat index, *HI*,

TABLE VII

Phase	m_v	m_r	m_{WC}	T	d	Phase	m_v	m_r	m_{WC}	T	d
	η Aquilae						δ Cephei				
0.0	3.70	3.20	3.65	5100°	0".0020	0.0	3.62	3.40	3.81	5500°	0".0016
.1	3.83	3.24	3.71	4900	.0021	.1	3.76	3.46	3.89	5300	.0017
.2	3.95	3.30	3.79	4800	.0022	.2	3.91	3.53	3.98	5100	.0017
.3	3.99	3.37	3.88	4600	.0022	.3	4.00	3.61	4.08	4900	.0018
.4	4.12	3.44	3.97	4500	.0022	.4	4.15	3.68	4.16	4800	.0018
.5	4.25	3.53	4.07	4400	.0022	.5	4.21	3.75	4.24	4800	.0018
.6	4.39	3.62	4.17	4400	.0022	.6	4.32	3.83	4.33	4700	.0018
.7	4.46	3.71	4.26	4400	.0021	.7	4.37	3.90	4.40	4700	.0017
.8	4.34	3.66	4.18	4500	.0020	.8	4.32	3.89	4.37	4800	.0016
0.9	3.98	3.42	3.90	4900	0.0020	0.9	3.97	3.64	4.07	5300	0.0015

TABLE VIII

Star	m_r	m_v	m_{pe}	m_b	*WC*	*HI*	From *WC*			
							HI	Type	T	d
η Aquilae:										
Max.	3.20	3.70	4.10	3.69	0.45	0.50	0.38	F7	5100°	0".0022
Min.	3.72	4.47	5.22	4.24	.55	.75	.56	gG3	4400	.0020
Range	0.52	0.77	1.12	0.55	.10	.25	.18	0.6 Sp. div.	700	.0002
δ Cephei:										
Max.	3.40	3.62	3.86	3.85	.41	.22	.30	F5	5500	.0018
Min.	3.92	4.38	4.98	4.43	.50	.46	.47	gG0	4700	.0015
Range	0.52	0.76	1.12	0.58	0.09	0.24	0.17	0.5 Sp. div.	800	0.0003

is the visual *minus* the radiometric magnitude. The data in the last four columns were obtained from the *WC;* the *HI* and the type from the observed relation[33] between them and *WC;* the temperature with the aid of Table II; and the diameters from equation (6). The ranges are for the maxima and minima of the individual quantities, which,

[33] *Mt. Wilson Contr.*, No. 369; *Astrophysical Journal*, **68**, 297, 1928, Table V.

except in the case of the diameters, practically coincide with the maxima and minima of light. The ranges between maximum and minimum in all these quantities are nearly the same for the two stars.

An interesting feature is the progressive increase in range from radiometric through visual to photoelectric magnitude. The visual range is about 0.24 mag. greater than the radiometric; and the photoelectric, about 0.36 mag. greater than the visual range. A simple extrapolation to λ 0.32 μ, which is the farthest to the violet that can be observed without interference by the variations of atmospheric ozone, shows that the range in this extreme violet region ought to be about 1.5 mag., an estimate confirmed by the temperature range, provided the stars behave as black bodies at this wave-length.

ALGOL

Since the entire primary eclipse of Algol covers about 9.7 hours,[34] 12 hours are required to include a significant part of the curve before and after eclipse. A continuous series of measures through minimum phase must therefore be made when the star is in opposition. Such series were made on November 16, 1923, and November 20, 1924. Since it is impractical to use the 100-inch telescope at an hour angle greater than 5.5 hours, and since the corrections for atmospheric absorption at large hour angles are uncertain, the measures were limited to a period of about 9 hours. The minimum phase was displaced from the middle of the observing interval on each night in such a manner as to cover the desired 12-hour interval.

The observing program consisted in alternate measures of the radiation from Algol and from ρ Persei throughout the night. A set of measurements included five deflections on the total radiation from Algol, five on the radiation transmitted by the water cell, five on that transmitted by a microscope cover-glass $\frac{1}{8}$ mm thick, and another five on the total radiation. The procedure in observing ρ Persei was the same except that no observations were made with the cover-glass screen. Occasional measures were also made on α Persei and β Andromedae as additional comparison stars. The average time required to obtain a complete set of measurements on Algol and its

[34] J. Stebbins, *Astrophysical Journal*, **53**, 105, 1921.

comparison star, yielding four complete determinations of the radiation from Algol, was 14.5 minutes. A fixed mirror placed close in front of the galvanometer mirror returned the light to the latter a second time before it reached the registering device, thus doubling the ordinary sensitivity of the galvanometer.[35] Both nights were clear, with fair seeing the first night and good seeing the second.

The magnitudes of Algol may be derived differentially with reference to the comparison star in the customary manner or by the method which we have used for the other variables. For the sake of homogeneity the latter method has been used. The atmospheric extinction was obtained from the measures of ρ Persei, the scale zero from the mean of the comparison stars, and the magnitude scale from the linear relationship of radiation to galvanometer deflection. ρ Persei was included as a comparison star, since Table V shows no definite variation in its radiometric magnitude.

The observations of Algol are given in Table IX. The epoch of observation, reduced to the sun, is Greenwich Mean Time. The phases have been computed from the minima at

$$\text{J.D.} = 2422619.7866 + 2^{d}.867301E ,$$

the epoch and period given by Stebbins.[34] The four determinations of radiometric magnitude from each set of measures are given together in the table: the first and last are from the free deflections; the second, from the deflection through the water cell corrected for the mean water-cell absorption of Algol, 0.23 mag.; and the third, from the deflection through the cover-glass corrected by 0.08 mag., the loss by reflection only, since the radiation reaching the thermocouple from this star is not appreciably absorbed by the glass. The fact that the magnitudes derived in this way from the deflection through water cell and cover-glass agree with the direct determination of radiometric magnitude is evidence that the difference in the temperatures of Algol and its companion is too small to be determined from the water-cell absorption. The data of Table IX are plotted in Figure 16, the observations of 1923 being represented by

[35] *Journal of the Optical Society of America*, 10, 267, 1925.

TABLE IX

ALGOL

Julian Day G.M.T.	Phase	m_r	Julian Day G.M.T.	Phase	m_r
1923 November 16					
242374..			242374..		
0.6434	−0.0899	2.23	0.8506	−0.0177	2.98
.6462	.0890	2.25	.8518	.0173	3.01
.6492	.0879	2.27	.8551	.0161	2.95
.....	.....	.....	.8573	.0153	3.05
.6672	.0816	2.20	.8706	.0107	3.12
.6695	.0808	2.20	.8729	.0099	3.12
.6718	.0800	2.17	.8753	.0091	3.10
.6741	.0792	2.17	.8776	.0083	3.10
.6864	.0749	2.20	.....	.....	.....
.6887	.0741	2.25	.8914	.0034	3.27
.6910	.0733	2.18	.8938	.0026	3.14
.6932	.0726	2.21	.8963	− .0017	3.37
.7084	.0673	2.19	.9083	+ .0025	3.44
.7108	.0664	2.20	.9106	.0033	3.22
.7130	.0657	2.20	.9129	.0041	3.21
.7153	.0649	2.21	.9152	.0049	3.40
.7256	.0613	2.26	.9285	.0095	3.42
.7278	.0605	2.22	.9308	.0103	3.26
.7301	.0597	2.28	.9331	.0111	3.14
.7323	.0589	2.25	.9353	.0119	3.17
.7434	.0551	2.31	.9478	.0162	3.05
.7458	.0542	2.35	.9503	.0171	3.13
.7483	.0533	2.30	.9530	.0180	3.00
.7504	.0526	2.38	.9552	.0188	3.13
.7623	.0485	2.36	.9663	.0227	2.94
.7646	.0477	2.38	.9687	.0235	2.89
.7670	.0468	2.42	.9713	.0244	2.90
.7694	.0460	2.42	.9735	.0252	2.87
.7831	.0412	2.47	.9850	.0292	2.74
.7853	.0404	2.49	.9876	.0301	2.81
.7878	.0396	2.56	.9898	.0309	2.76
.7901	.0388	2.54	0.9918	.0316	2.72
.8008	.0350	2.62	1.0060	.0365	2.70
.8032	.0342	2.63	1.0084	.0374	2.70
.8055	.0334	2.64	1.0108	.0382	2.59
.8078	.0326	2.69	1.0128	+0.0389	2.63
.8280	.0255	2.83			
.8304	.0247	2.68			
.8329	.0238	2.79			
0.8354	−0.0230	2.84			

TABLE IX—*Continued*

Julian Day G.M.T.	Phase	m_r	Julian Day G.M.T.	Phase	m_r
		1924 November 20			
242411..			242411..		
0.6384	−0.0505	2.16	0.8213	+0.0133	3.03
.6408	.0496	2.35	.8243	.0144	3.11
.6431	.0488	2.42	.8275	.0155	2.97
.6455	.0480	2.21	.8302	.0164	2.97
.6741	.0380	2.44	.8490	.0230	2.86
.6767	.0371	2.53	.8513	.0238	2.80
.6793	.0362	2.58	.8535	.0245	2.81
.6819	.0353	2.41	.8559	.0254	2.73
.6991	.0293	2.68	.9109	.0446	2.37
.7019	.0283	2.71	.9123	.0451	2.36
.7040	.0276	2.77	.9156	.0462	2.38
.7067	.0267	2.72	.9183	.0471	2.45
.7224	.0212	2.70	.9395	.0545	2.32
.7249	.0203	2.86	.9417	.0553	2.28
.7276	.0194	2.91	.9439	.0561	2.30
.7300	.0185	2.78	.9466	.0570	2.28
.7458	.0130	3.16	.9598	.0616	2.37
.7484	.0121	3.05	.9627	.0626	2.18
.7507	.0113	3.08	.9648	.0634	2.26
.7532	.0104	3.13	.9675	.0643	2.20
.7690	.0049	3.21	.9941	.0736	2.25
.7713	.0041	3.22	.9962	.0743	2.19
.7739	.0032	3.18	0.9986	.0751	2.25
.7762	−0.0024	3.39	1.0012	+0.0761	2.21
.7967	+0.0047	3.16			
.7993	.0056	3.16			
0.8017	+0.0065	3.18			

circles and those of 1924 by squares. The full line is the radiometric curve representing the mean of both series, normal places for which are indicated by large circles. The broken line is the light-curve determined by Stebbins with a selenium cell and a photoelectric cell, both of which give essentially the same curve.

Table X gives the radiometric and photoelectric magnitudes just before and just after eclipse and at minimum, with their ranges.

The photoelectric range is 0.12 mag. greater than the radiometric; and the photoelectric magnitude is fainter than the radiometric, not only at mid-eclipse where the difference is greatest, but through-

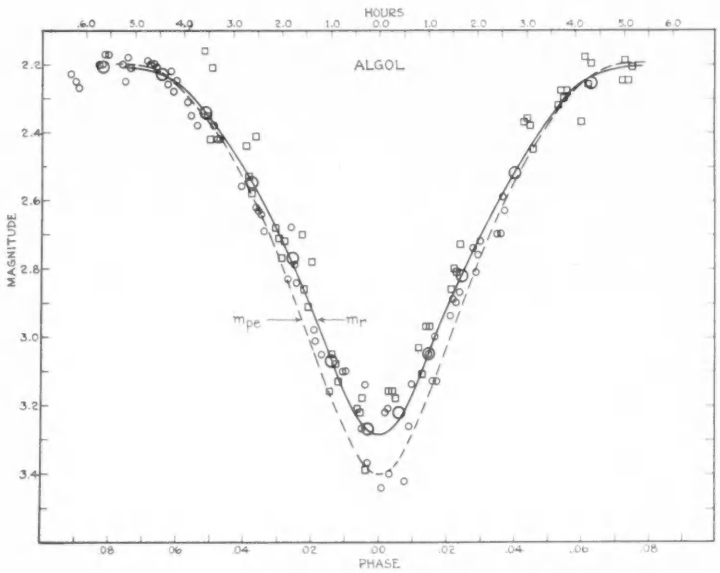

FIG. 16.—Radiation-curve of Algol

TABLE X

	m_r	m_{pe}
Mag. before and after eclipse	2.21	2.20
Mag. at minimum	3.29	3.40
Range	1.08	1.20

out the period of occultation—a circumstance probably due indirectly to the lower temperature of the occulting star, although the temperature difference is too small to be detected from the water-cell absorption.

The observed epoch of minimum phase, J.D. 2424110.7880, was 0.0017 period, or 7 minutes later than that computed. This differ-

ence in phase may be removed by using a mean period of $2^{d}.867310$ for the four-year interval between the photoelectric and the radiometric measures.

We wish to acknowledge the assistance of Miss M. L. Richmond in measuring the photographically recorded deflections and in the rather involved processes of reduction.

CARNEGIE INSTITUTION OF WASHINGTON
MOUNT WILSON OBSERVATORY
June 1933

THE TITANIUM OXIDE AND ZIRCONIUM OXIDE BANDS IN STELLAR SPECTRA[1]

By R. S. RICHARDSON

ABSTRACT

The percentage of *ZrO* and *TiO* molecules dissociated at different temperatures and pressures has been calculated. The behavior of the *ZrO* and *TiO* bands in S- and M-type spectra is discussed on the basis of these calculations.

One of the most interesting results that may be obtained when the analysis of a molecule has been made and its heat of dissociation is known is the degree of dissociation of the components at different temperatures and pressures. The recent investigation of the zirconium oxide (*ZrO*) and titanium oxide (*TiO*) bands by F. Lowater[2] and A. Christy,[3] respectively, supplies the data necessary to interpret the behavior of these compounds in stellar spectra.

The equation of dissociation equilibrium for molecules is[4]

$$\log K=\frac{-5041D}{T}+\tfrac{3}{2}\log T+\tfrac{3}{2}\log M+\log G$$
$$+\log\left(1-e^{\frac{-h\nu}{RT}}\right)-\log I-39.688\,. \quad (1)$$

The constants in (1) for *ZrO* were obtained as follows:

K, the equilibrium coefficient, is equal to $p_{Zr}p_O/p_{ZrO}$, where p is the partial pressure of the components indicated. Let x be the fraction of *ZrO* molecules dissociated and P the sum of the partial pressures of the reacting substances, then

$$K=\frac{Px^2}{1-x^2}\,.$$

D, the heat of dissociation, was calculated by the method of Birge and Sponer,[5] which involves an extrapolation from the observed vi-

[1] *Contributions from the Mount Wilson Observatory, Carnegie Institution of Washington*, No. 479.

[2] *Proceedings of the Physical Society of London*, **44**, 51, 1932.

[3] *Astrophysical Journal*, **70**, 1, 1929.

[4] *Ibid.*, p. 8.

[5] *Physical Review*, **28**, 259, 1926.

brational levels to the unobserved limiting level at which the interval between consecutive levels would vanish. The expression used is

$$D=\frac{\omega_e^2}{4\omega_e x_e}-\tfrac{1}{2}\,\omega_e\,, \qquad (2)$$

where ω_e is the frequency (cm^{-1}) of vibrations of the nuclei with infinitesimal amplitude about their equilibrium positions, and x_e is a small constant which takes into account the fact that the vibrations of the nuclei are anharmonic. For the lower level of *ZrO* these constants are, with sufficient accuracy, $\omega_e=940$ cm^{-1} and $\omega_e x_e=3.5$ cm^{-1}. The corresponding value for the heat of dissociation is $D=7.5$ volts.

G is given by the expression $g_{Zr}g_O/g_{ZrO}$, where $g=\sum(2J+1)$ for all levels of a multiplet. For an atom, J, the total quantum number, is equal to $L-S$, $L-S+1$, $L-S+2$, ... $L+S$, where L and S are, respectively, the quantum numbers for the orbital and spin angular momenta. The values of J are indicated by subscripts on the right of the term symbol. Since the lowest state of *Zr* is ${}^3F_{2,3,4}$, $g_{Zr}=5+7+9=21$. The lowest state of oxygen is ${}^3P_{0,1,2}$, therefore $g_O=9$. The lowest state of *ZrO* is ${}^3\Pi$, and the corresponding quantities for this molecule are $\Lambda=1$, $S=1$, so that $J=2$, 1, 0, giving $g_{ZrO}=9$. Hence $G=21$.

I, the moment of inertia of a molecule, is found from a rotational or fine-structure analysis of the band system. Such an analysis is not available for *ZrO*, but a moderately accurate estimate of I can be obtained from an empirical relation discovered by P. M. Morse,[6] namely,

$$r_e^3\,\omega_e \sim \text{Const.}\,, \qquad (3)$$

where r_e is the distance between the nuclei in their equilibrium position. Equation (3) holds fairly well for a wide variety of electronic states, even of different molecules. For molecules composed of two atoms having nearly the same atomic weight, the constant has the value 3×10^{-21} cm^2. If the atoms differ considerably in atomic weight, as in the case of the hydrides, the constant may be as large as 6×10^{-21} cm^2. The writer has computed values of $r_e^3\omega_e$ for all the metallic oxides

[6] *Ibid.*, **34**, 57, 1929.

for which these quantities are known. By plotting these results against the logarithms of the atomic weights of the metals, a roughly linear relation was obtained. This process gave for *ZrO*, $r_e^3\omega_e = 4.5 \times 10^{-21}$, from which r_e can be found, since ω_e is known. The moment of inertia is defined by

$$I = \mu r_e^2 , \tag{4}$$

where μ is the reduced mass of the molecule.[7] Substitution of numerical values into (4) gives for *ZrO*, $I = 64 \times 10^{-40}$ gm. cm^2.

The other constants in (1) are: ν, which for the $^3\Pi$ state of *ZrO* equals $\omega_e c$, where c is the velocity of light; in this case, $\nu = 2.8 \times 10^{13}$ sec.$^{-1}$, approximately.

$$M = \frac{M_{Zr} M_O}{M_{ZrO}} ,$$

in which the various M's represent the masses of the components in gram mols; and finally, T equals absolute temperature.

Insertion of numerical values into (1) gives for the final working equation

$$\log \frac{x^2}{1-x^2} = \frac{-37{,}800}{T} - \log P + \tfrac{3}{2} \log T + \log \left(1 - e^{-\frac{1340}{T}}\right) + 1.53 . \tag{5}$$

The heat of dissociation is by far the most important constant involved in (5), since a small error in D will make a large error in x. The value of 7.5 volts for *ZrO* is necessarily quite uncertain, but, when compared with 6.74 volts given by Christy[8] for *TiO*, appears to be of about the right order of magnitude. All the observational evidence available indicates that *ZrO* is more stable at high temperatures than *TiO*. P. W. Merrill[9] states that ". . . . in general the temperature range for the production of the zirconium bands is higher than that for the titanium bands." Likewise, A. S. King's[10] investigation of *ZrO* and *TiO* in the electric furnace showed that ". . . . the

[7] See W. Jevons, *Report on Band-Spectra of Diatomic Molecules*, p. 24, 1932, for details in the calculation of μ.

[8] *Op. cit.*, p. 7.

[9] *Mt. Wilson Contr.*, No. 325; *Astrophysical Journal*, **65**, 45, 1927.

[10] *Publications of the Astronomical Society of the Pacific*, **36**, 140, 1924.

zirconium bands belong to the oxide and their presence indicates a distinctly higher temperature stage than that required for the bands of titanium oxide."

Equation (5), together with the corresponding equation for *TiO* given by Christy,[11] furnishes a basis for interpreting the behavior of *ZrO* and *TiO* bands in stellar spectra. The principal observational facts[12] are as follows:

Stars of Class S.—The *ZrO* and *TiO* bands occur simultaneously in stars of class S. In the variables, the *ZrO* bands are present during all or most of the light-cycle, being slightly weaker near maximum, when the star is presumably at a higher temperature. The *TiO* bands are either absent or extremely weak at maximum, but may be strong when the variable is fainter.

Stars of Class M.—The *TiO* bands occur alone in this class, and in the later divisions completely dominate the spectrum. The temperatures of the M and S stars probably overlap. Several lines of inquiry indicate that the S-type stars are probably lower in density than those of class M.

Figure 1*a* shows the percentage of *TiO* and *ZrO* dissociated at different temperatures for a constant pressure of 10^{-6} atmospheres; Figure 1*b*, the percentage dissociated at different pressures for a constant temperature of 2500°. It is clear from Figure 1*a* that as a variable star approaches maximum and the temperature increases, the *TiO* is rapidly dissociated and disappears from the spectrum at about 3000°. The *ZrO* decreases slightly in intensity, but not nearly so much as the *TiO;* for when *TiO* is about to disappear, *ZrO* is only about 60 per cent dissociated. Similarly, Figure 1*b* shows that *TiO* is much more sensitive to pressure changes than *ZrO*, and cannot exist at a temperature of 2500° if the pressure falls below 10^{-8} atmospheres. Since in the atmosphere of a variable star the temperature and pressure probably vary simultaneously, the effects produced in the band spectrum may be very complex. The simple theory outlined here, however, seems adequate to account for the general nature of the spectral changes.

The fact that *TiO* alone is found in M-type stars can be explained if their density is greater than stars of class S, as indicated by the

[11] *Op. cit.*, p. 8. [12] Merrill, *Op. cit.*, p. 41.

observations. Suppose the pressure and temperature in the atmosphere of a star to be 10^{-4} atmospheres and 2500°, respectively. By referring to Figure 1*b*, it is seen that neither *TiO* nor *ZrO* is appreciably dissociated, so that the two compounds would compete on a more

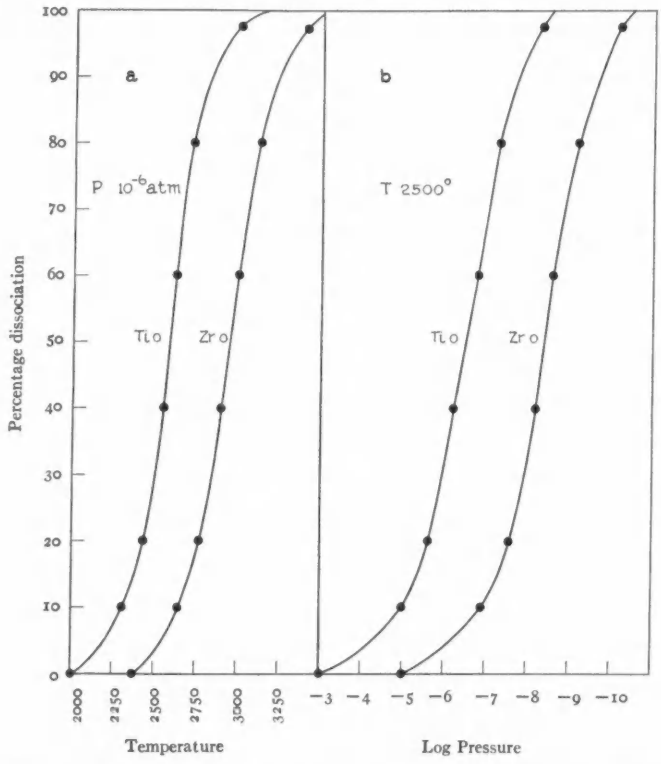

FIG. 1.—Diagrams showing the percentages of *TiO* and *ZrO* dissociated at different temperatures and pressures.

nearly equal basis. But as the vast difference between the amount of *Ti* and *Zr* present in stellar atmospheres greatly favors the formation of *TiO* over *ZrO*, the band spectrum of *TiO* would still be by far the more prominent spectral feature.

CARNEGIE INSTITUTION OF WASHINGTON
MOUNT WILSON OBSERVATORY
June 1933

A PHOTOMETRIC STUDY OF SUN-SPOTS AND FACULAE[1]

By R. S. RICHARDSON

ABSTRACT

The intensities of sun-spots and faculae at different distances from the center of the sun's disk, relative to the intensity of the surrounding photosphere, have been determined from the direct photographs of the sun taken at Mount Wilson since 1925. The photographs were calibrated by assuming that the intensity across the disk for the effective wave-length of the plate corresponds to that given by Abbot. Direct standardization of plates of the same brand by diaphragming the objective shows that on the average they do not differ from Abbot's intensities by more than 4 per cent.

The measurements on sun-spots indicate that the ratio of intensity of any part of the spot to that of the surrounding photosphere is independent of the distance from the center of the disk. The observations can be represented better by assuming that sun-spots are in radiative rather than in adiabatic equilibrium.

The relation between the intensity and the area of sun-spots was investigated by measuring the intensity of the penumbra in fifteen spot groups. The areas of the individual spots, corrected for foreshortening, ranged from 78 to 2860 millionths of the sun's visible hemisphere. The logarithms of the areas plotted against the intensity ratios, penumbra/photosphere, indicate a roughly linear relation.

The intensity of the faculae relative to the surrounding photosphere was measured at various points between 0.60–0.95 of the distance from the center of the disk to the limb. Minnaert and Wanders have advanced a theory of the faculae based on the fact that a rising column of gas expanding adiabatically will be brighter than its surroundings if the ratio of the specific heats is less than 1.33. A fair agreement with the observations can be obtained by assuming a ratio of specific heats equal to 1.14.

1. INTRODUCTION

Sun-spots are commonly explained as regions of relatively low temperature produced by gases rising in a vortex and cooling by adiabatic expansion.[2] The general acceptance of this explanation is remarkable, because most of the direct observational evidence is rather unfavorable to it. For example, it does not account naturally for the most striking characteristic of sun-spots, namely, the sharp boundaries between the umbra, penumbra, and photosphere. Another difficulty is the absence of measurable upward velocities in the umbra. But it is difficult to abandon the adiabatic hypothesis,

[1] *Contributions from the Mount Wilson Observatory, Carnegie Institution of Washington*, No. 480.

[2] H. N. Russell, *Mt. Wilson Contr.*, No. 217; *Astrophysical Journal*, **54**, 293, 1921; V. Bjerknes, *Mt. Wilson Contr.*, No. 312; *Astrophysical Journal*, **64**, 93, 1926; S. Rosseland, *Mt. Wilson Contr.*, No. 313; *Astrophysical Journal*, **63**, 356, 1926; R. M. Petrie, *Monthly Notices of the Royal Astronomical Society*, **90**, 480, 1930; E. A. Milne, *ibid.*, **90**, 487, 1930; A. Unsöld, *Zeitschrift für Astrophysik*, **1**, 138, 1930; **2**, 209, 1931.

because it is practically the only process known sufficiently powerful to produce the relatively low temperatures observed in sun-spots.[3]

In their recent work on the theory of sun-spots, Minnaert and Wanders[4] have discussed in detail two important consequences of the adiabatic theory which can be compared directly with observation: (1) the ratio of intensity between spot and photosphere for different wave-lengths and (2) the ratio of intensity between spot and photosphere at different positions on the disk. In accordance with the usage of Minnaert and Wanders, (1) will hereafter be called the "wave-length variation" and (2) the "angle variation." Minnaert and Wanders found that the adiabatic theory fails completely to represent observations for the wave-length variation. They were unable to test the adiabatic theory for the angle variation because the observational data then available were very poor. In order to provide data suitable for comparison with theory, the intensities of sun-spots and faculae at different distances from the center of the disk have been measured relative to the intensity of the surrounding photosphere. These data are presented in this paper and compared with theory, together with several by-products of the measurements.

2. OBSERVATIONAL MATERIAL

The observational material was obtained mostly from the direct photographs of the sun taken at Mount Wilson since 1925 as a part of the routine solar work. Since two photographs are taken on every clear day, it was possible to select from the large number of plates available only those of the finest quality. The diameter of the solar image on these plates is about 17 cm (6.5 in.). Two types of plate, sensitive to different spectral regions, have been used: (*a*) Contrast Bromide plates, very high in contrast, taken without a filter, the effective wave-length being λ 4330; (*b*) Yellow-Green Sensitive plates, also very high in contrast, used with an orange filter, the effective wave-length of plate and filter being λ 5780.

[3] V. A. Ambarzumian and N. A. Kosirev, *Astronomische Nachrichten*, **233**, 107, 1928; E. Pettit and S. B. Nicholson, *Mt. Wilson Contr.*, No. 397; *Astrophysical Journal*, **71**, 153, 1930; R. S. Richardson, *Mt. Wilson Contr.*, No. 422; *Astrophysical Journal*, **73**, 216, 1931; C. E. Moore, *Mt. Wilson Contr.*, No. 446; *Astrophysical Journal*, **75**, 222, 1932.

[4] *Zeitschrift für Astrophysik*, **5**, 297, 1932.

In addition, several photographs of a large sun-spot were taken especially for this investigation at the 150-foot tower telescope where the diameter of the solar image is about 425 mm. These were exposed behind a red filter on a plate of moderate contrast, Slow Panchromatic C. The effective wave-length of the plate and filter is λ 6450.

The Contrast Bromide and Yellow-Green Sensitive plates were not standardized when taken. The only means of calibrating them is to assume that the intensity across the disk for the effective wave-length of the plate corresponds to that given by Abbot's[5] bolometric measurements. A portion of the characteristic curve which includes the penumbrae and faculae is thus obtained for each plate. Intensities for the umbrae could be found only by extrapolating Abbot's measurements out to the limb, where the intensity was taken to be zero.

In order to find how closely the distribution of intensity across the direct photographs really conforms to Abbot's measurements, four Contrast Bromide and four Yellow-Green Sensitive plates were exposed in the usual way and standardized directly by diaphragming the objective. The intensity distribution for each plate was then found from four series of nine readings each across the disk in four directions 90° apart. On the average, no single series of intensities differed from Abbot's by more than 4 per cent.

The influence of an error of 4 per cent on the final results was investigated by determining the intensities of the penumbra from a series of disk intensities which differed from Abbot's on the average by this amount. A comparison with the intensities of the penumbra based on Abbot's measurements gave the results shown in Table I. The two sets of intensities differ systematically by an average of about 2 per cent. A reduction from Abbot's intensities to the Mount Wilson values would be hazardous, however, since we have no assurance that plates taken several years ago would show the same systematic difference in intensity as those used for the test. The most that can be said is that the intensities of the sun-spots given later on are probably not in error on the average by amounts greater than those shown in Table I.

[5] *Annals of the Astrophysical Observatory of the Smithsonian Institution*, **3**, 159, 1913.

The Slow Panchromatic C plates were standardized over the desired range of intensity by diaphragming the objective at the time they were exposed.

An ideal set of plates for this investigation would consist of daily photographs taken during good seeing of a large sun-spot as it passes across the disk. The importance of the definition must be emphasized, for it is the most serious source of error present. Unsteadiness of the image scatters light into the sun-spot and tends always to make its intensity approach that of the photosphere. Hence, intensity measurements of a sun-spot as it moves across the disk will be misleading unless made under uniformly good seeing conditions.

TABLE I

Plate	sin θ	Intensity $\frac{\text{Penumbra}}{\text{Photosphere}}$	Mt. W. − Abbot
		Mt. Wilson	
P 7287*a*	0.76	0.87	+0.04
7287*b*	.76	.86	+ .06
7508	.79	.84	.00
7509	.63	.78	− .01
7288	.60	.77	.03
7293	.58	.71	.03
7292	.39	.72	.02
7290	.29	.72	.06
7291*a*	.26	.64	.08
7291*b*	.26	.72	.03
7511	0.26	0.74	−0.04

Among about forty-eight hundred photographs of the sun taken at Mount Wilson since 1925, a series of nine Contrast Bromide and eight Yellow-Green Sensitive plates were found that satisfied all the requirements. These seventeen plates form the principal basis for the study of the angle variation for sun-spots. The study of the angle variation for faculae is also based on these plates and, further, upon several isolated plates which have been given equal weight. In addition, ten plates of high quality were measured to investigate a possible relation between the area and relative blackness of sun-spots. The Slow Panchromatic C plates were used primarily to obtain the distribution of energy over a sun-spot.

3. REDUCTION OF OBSERVATIONAL MATERIAL

The photographic density of the sun-spots was determined from tracings made with the Koch registering microphotometer. The reduction of a plate was effected by making a drift-curve across the spot from the center of the disk to the limb. Abbot's intensities across the disk were extrapolated outward from 95 to 100 per cent of the solar radius and plotted against the corresponding densities found from the drift-curve. Although the characteristic curves thus obtained are satisfactory in appearance, it must be remembered that the extrapolation is large and rather arbitrary in character. The densities of the sun-spots were measured from tracings twenty times the scale of the drift-curves, and the corresponding intensities were read from the characteristic curves already found.

The densities of the faculae were obtained from direct scale readings of galvanometer deflections. The density across the disk was derived from readings taken on either side of the faculae up to distances of 95 per cent of the solar radius outward. The characteristic curve of the plate was then determined as before by plotting the densities against Abbot's intensities. It was unnecessary to extrapolate this curve in order to find the intensities of the faculae.

After the intensities for the spots or faculae had been measured by the methods just described, they could be referred to the surrounding photosphere either by measuring directly the density near the given object and then reading the intensity off the characteristic curve or by assuming the intensity at this point on the disk to be the same as that given by Abbot. Both methods were used and gave concordant results.

4. THE ANGLE VARIATION FOR SUN-SPOTS

Figure 1 shows the contours of two sun-spots at different distances from the center of the disk for effective wave-lengths of λ 4330 and λ 5780.

The contours for λ 4330 were made on spot No. 9637 of the Greenwich series which appeared in latitude $+15^{\circ}.6$ and had a maximum area on April 30, 1925, of 883 millionths of the sun's visible hemisphere. The contours for λ 5780 were made on Greenwich No. 11280, latitude $-6^{\circ}.9$. The maximum area of this spot occurred on August

13, 1930, when it equaled 382 millionths of the sun's visible hemisphere. All intensities are in terms of the photosphere surrounding the sun-spot. A precise comparison between consecutive contours is impossible owing to differences in seeing and actual changes in the spot itself from day to day. If allowance is made for these sources of disturbance, the intensities of different parts of the spot relative to the surrounding photosphere are practically unchanged.

An attempt has been made to represent these intensities by assuming that the sun-spot is in (*a*) adiabatic equilibrium and (*b*) radiative

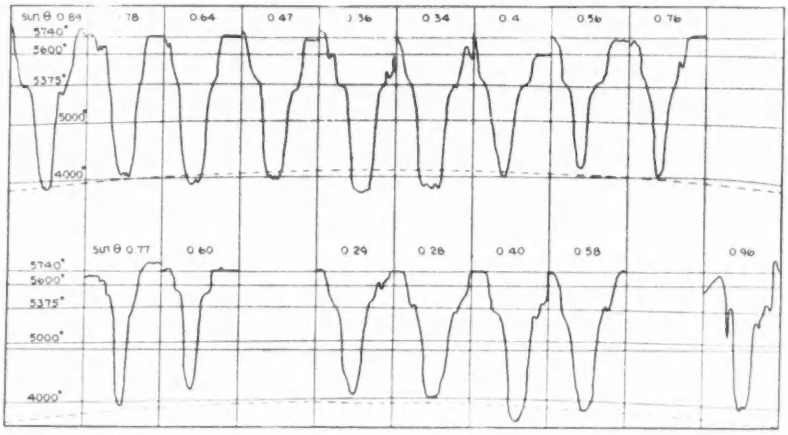

FIG. 1.—Contours above are of Greenwich sun-spot No. 9637, for an effective wave-length of λ 4330; below, for Greenwich spot No. 11280, for an effective wave-length of λ 5780.

equilibrium. The photosphere in both cases is assumed to be in radiative equilibrium at an effective temperature of 5740° K. Only the actual working equations will be given here, since a detailed treatment has been published in Minnaert and Wanders' paper.

a) *Adiabatic equilibrium.*—The spot is supposed to originate at some optical depth τ_0 where the temperature is T_0. The optical depth τ is connected with the density ρ, the mass coefficient of absorption for unit density, k, and the vertical depth, x, in the sun by the relation

$$k\rho dx = d\tau \,, \tag{1}$$

where k is assumed to be constant. A ray traveling at an angle θ to the vertical must traverse an optical thickness τ sec θ before emer-

gence and be reduced by absorption to the fraction $e^{-\tau \sec \theta}$ of its original intensity. The total radiation from the spot for a given wave-length will then be

$$J_\lambda^{ad}(\tau, \theta) = \frac{c_1}{\lambda^5} \int_0^{\tau_0} \frac{e^{-\tau \sec \theta} \sec \theta \, d\tau}{e^{\frac{c_2}{\lambda T_{ad}}} - 1}, \tag{2}$$

where

$$T_{ad} = C\tau^{\frac{\gamma-1}{\gamma}}, \tag{3}$$

$$C = T_0 \tau_0^{\frac{1-\gamma}{\gamma}}, \tag{4}$$

and

$$T_0 = 5740 \sqrt[4]{\tfrac{1}{2}} (1 + \tfrac{3}{2}\tau_0)^{\frac{1}{4}}. \tag{5}$$

In these equations, γ is the ratio of the specific heats of the gas, c_p/c_v; $c_1 = 3.697 \times 10^{-5}$ erg cm^2 sec.$^{-1}$; and $c_2 = 1.432$ cm deg. For the photosphere, the corresponding relation is

$$J_\lambda^{rad}(\tau, \theta) = \frac{c_1}{\lambda^5} \int_0^{\infty} \frac{e^{-\tau \sec \theta} \sec \theta \, d\tau}{e^{\frac{c_2}{\lambda T_{rad}}} - 1}, \tag{6}$$

where

$$T_{rad} = 5740 \sqrt[4]{\tfrac{1}{2}} (1 + \tfrac{3}{2}\tau)^{\frac{1}{4}}. \tag{7}$$

The ratio of intensities of spot and photosphere at different distances from the center of the disk can now be obtained by calculating $J_\lambda^{ad}(\tau, \theta)/J_\lambda^{rad}(\tau, \theta)$ for different values of θ. The procedure is first to assume a value for τ_0 and from it compute all the quantities necessary for the evaluation of $J_\lambda^{ad}(\tau, \theta)$. The numerical values of the integrals (2) and (6) were found by graphical integration. In practice, the computation of (6) was carried only to $\tau = 10$.

The broken curve in Figure 1 shows the ratio of intensity, spot/photosphere, for different values of sin θ and for a value of $\gamma = 5/3$ for a monatomic gas. The adiabatic theory requires the intensity of the umbra relative to the photosphere to fall appreciably near the limb. The observed contours give no definite indication of such a

change, but the discrepancy is well within the errors of observation. A more serious difficulty is that the penumbra is not explained by the adiabatic theory. The only adjustable quantity in (1), (2), (3), and (4) is τ_0, for which there is no value, however large, which will give intensities for the penumbra as large as those observed.

b) *Radiative equilibrium.*—Minnaert and Wanders were unable to obtain agreement with observation by modification of the adiabatic theory. They finally abandoned it entirely, and assumed instead that the umbra is in pure radiative equilibrium at an effective temperature of 4300° K. This assumption gives a much better representation of the observations than any that could be obtained on the basis of adiabatic equilibrium. The same method has been tried here with satisfactory results. The continuous curves in Figure 1 indicate the ratio of intensity, spot/photosphere, corresponding to radiative equilibrium at temperatures of 4000°, 5000°, 5375°, and 5600° K. The theory of radiative equilibrium also requires that this ratio decrease near the limb, but by an amount so small as to make it almost impossible of detection. Since the observed values of the ratio for different parts of a spot seem to remain practically unchanged as the spot passes across the disk, the theory of radiative equilibrium accords well with the observations. Hence, the present investigation of the angle variation agrees with Minnaert and Wanders' work on the wave-length variation and is favorable to their conclusion that a satisfactory agreement between theory and observation of sun-spots cannot be obtained on the basis of adiabatic equilibrium.

There is, however, an apparent disagreement with the results of N. Barabascheff and B. Semejkin,[6] who have studied photometrically twenty-five spots that appeared between May 22, 1931, and August 2, 1931. They used a solar image 141 mm in diameter and a plate and filter giving an effective wave-length of about λ 6000. The plates were calibrated by means of a tube densitometer. The intensity of the umbra was determined with respect to the surrounding photosphere, and its temperature calculated from Planck's formula. The spots were then grouped according to their distances from the center of the disk, and the mean intensity and temperature found for

[6] *Zeitschrift für Astrophysik*, **5**, 54, 1932.

each group. The measurements show that the intensity of the umbra relative to the photosphere increases[5] from about 0.24 at $\sin\theta = 0.10$ to 0.54 at $\sin\theta = 0.90$.

It may be remarked, however, that if the logarithms of the areas of these spots are plotted against the intensity ratio, umbra/photosphere, a curve similar to Figure 3 is obtained. A plot of the areas of the individual spots against $\sin\theta$ also shows a rough linear relation.

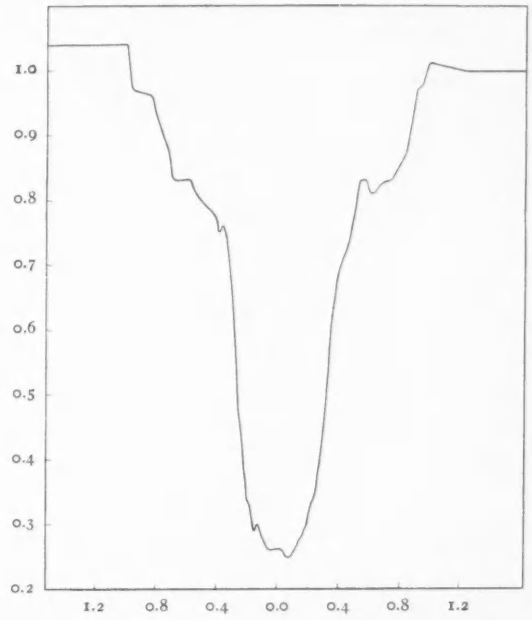

FIG. 2.—Contour of Mount Wilson sun-spot No. 4362. The ordinates give the intensity of the sun-spot in terms of the photosphere as unity. The abscissae indicate fractional distance from the center of the spot.

Hence, the observed increase in intensity may be simply an accidental result due to the selection of material. Another possibility is that many of the spots appear to be rather small for accurate photometric work. Unless a spot is quite large, it is difficult to keep the beam of light in the microphotometer from overlapping the penumbra and thus making the intensity of the umbra too high. This source of error becomes increasingly serious toward the limb, owing to the diminution in size of the spot produced by foreshortening.

Figure 2 is a contour of Mount Wilson spot No. 4362 in latitude

$-9°$ for August 3, 1932, during good seeing, at a distance from the center of the disk corresponding to sin $\theta = 0.36$. The spot had an area of 200 millionths of the sun's visible hemisphere. It was photographed on a Slow Panchromatic C plate with a red filter, the effective wave-length of the combination being λ 6450. The plate was calibrated over the entire range of intensity in the sun-spot by diaphragming the objective. The scale of ordinates on the left gives the intensity of the spot relative to the surrounding photosphere; the abscissae give the fractional distance from the center of the umbra.

It is difficult to abandon the adiabatic hypothesis entirely because, as already mentioned, it is almost the only process known sufficiently powerful to account for the relatively low temperatures in sun-spots. Minnaert and Wanders have suggested that the initial cooling in a sun-spot may be produced so far below the surface that the overlying gases which compose the umbra and penumbra are practically in radiative equilibrium. This view explains the absence of upward velocities in the umbra, but the origin of the Evershed effect in the penumbra is not obvious. It is also consistent with the fact that, although a magnetic field exists in sun-spots at the level of the umbra, no vortical motion has been observed to produce it.

5. RELATION BETWEEN THE INTENSITY AND THE AREA OF SUN-SPOTS

It has been stated that the temperatures of all sun-spots are about the same,[7] although the observational evidence for this assertion is not given. In order to obtain data on this subject, the intensity of the penumbra was measured by the methods previously described in fifteen spot groups at distances from the center of the disk ranging from 18 to 80 per cent of the solar radius. The areas of individual spots, taken from the *Greenwich Photoheliographic Results* and corrected for foreshortening, ranged from 78 to 2860 millionths of the sun's visible hemisphere.

Figure 3 shows the curve obtained by plotting the logarithms of the areas as ordinates against values of the intensity ratio, penum-

[7] Unsöld, *Zeitschrift für Astrophysik*, **2**, 209, 1931; H. N. Russell, *Scientific American*, **144**, 302, 1931.

bra/photosphere. Although the points are scattered, the linear relation

$$\log A = 4.800 - 3.544R\,, \tag{8}$$

is fairly well defined, A being the total area of the spot in millionths of the visible hemisphere and R the intensity ratio.

This relationship may be only apparent, however, for poor seeing probably increases the intensity of small spots relative to that of large spots. On our plates the penumbrae of small spots are often less than a millimeter across, while many of the large spots have pe-

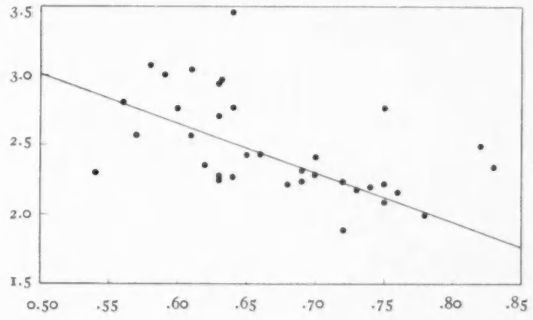

FIG. 3.—Relation between the log area of sun-spots (ordinates), and the intensity ratios, penumbra/photosphere (abscissae).

numbrae as much as 3 mm across. Hence, there must be considerable difference between the relative amounts by which large and small sun-spots are affected by scattered photospheric light.

Another possible source of error lies in the measurements themselves. The cross-section of the beam of light in the densitometer may extend, for example, over 80 per cent of the width of the penumbra of a small spot, but over only 40 per cent of that of a large spot. Measurements of density in the two cases do not, therefore, refer to the same portions of the penumbra. This source of error was checked by measuring the intensities of spots first with a beam of light of fixed diameter and then with light-beams having cross-sections proportional to the areas of the spots. Both methods gave the same result within the errors of observation. It is likely that the cross-section of the beam of light is unessential so long as it is completely enclosed by the penumbra.

6. INTENSITIES OF THE FACULAE

Measurements on the faculae were confined to the Contrast Bromide and Yellow-Green Sensitive plates. The faculae can be detected on these plates with reasonable certainty only at distances from the limb of about 40 per cent or less of the solar radius. The individual intensities derived fluctuate widely, owing to actual differences in the brightness of the faculae themselves. These random variations can be smoothed out by taking a large number of readings. A more troublesome source of error arises from the difficulty

TABLE II

Distance from Center of Disk	Int. Faculae to Photosphere		O−C	
	λ 4330	λ 5780	λ 4330	λ 5780
0.60	1.04	1.02	−0.10	−0.06
.70	1.06	1.03	.11	− .05
.80	1.10	1.04	.08	− .05
.90	1.14	1.10	.05	+ .01
0.95	1.17	1.16	−0.02	+0.07

of setting the beam of light on the faculae without including some of the disk as well. This disturbance is especially serious away from the limb, where it is practically impossible to distinguish between faculae and disk. For this reason, the measured intensities given in Table II are probably too small.

The only attempt to account for the faculae that the author has found is one given by Minnaert and Wanders.[8] Their explanation arises from a discussion of the effect that a variable absorption coefficient would have on a column of gas rising and expanding adiabatically. They arrive at the interesting result that such a column will be darker or brighter than its surroundings according to whether the ratio of the specific heats, γ, is greater or less than $4/3$, and think it probable that the influence of irradiation and recombination may produce an "effective" γ in limited regions which is less than $4/3$.

[8] *Op. cit.*, p. 309.

The data in Table II have been represented on this basis, by using equations (1), (2), (3), and (4) as before, except that γ, as well as τ_0, is now an independent variable. The best representation was obtained for $\tau_0 = 3$ and $\gamma = 1.14$. The computed values are mostly larger than those observed, but the discrepancy may arise from the fact that the latter, as explained above, are probably too small.

CARNEGIE INSTITUTION OF WASHINGTON
MOUNT WILSON OBSERVATORY
August 1933

NOTES

NOTE CONCERNING THE SPECTRUM OF NOVA OPHIUCHI NO. 3 (RS OPHIUCHI)

ABSTRACT

The observed positions of emission and the relative intensities of spectral lines in Nova Ophiuchi No. 3 are given from measurements of three spectrograms obtained with an objective-prism camera having an average dispersion of about 100 A/mm.

On August 18.12, 24.14, and 29.14, 1933, G.C.T., spectrograms were obtained with a 6-inch reflector and a 30° objective prism having a dispersion such that the distance between $H\beta$ and $H\epsilon$ is approximately 8.8 mm. Measurements of the hydrogen lines were used to form a dispersion-curve from which the wave-lengths of all other spectral lines were interpolated graphically. The observed positions

TABLE I

August 18.12	August 24.14	August 29.14	Identification
4101 (10)	4101 (10)	4101 (10)	*Hδ*§
4172 (2)			*Fe* II
4232 (2)			*Fe* II
4302 (3) *W**			*Fe* II(?)
4340 (15)	4340 (15)	4340 (15)	*Hγ*
4380 (3)†	4377 (3) *A–R*	4364 (1)	*He* I; *Fe* II
		4392 (3) *A–V*	
4408 (3)			
4462 (4) *A–R*	4464 (6)	4476 (4) *A–V*	*He* I
	4484 (2)		
4507 (4)	4511 (3)	4518 (1)	*Fe* II
4548 (4)	4547 (4) *SlA–R*	4557 (1)	*Fe* II
4576 (5)	4578 (5)	4587 (1)	*Fe* II
4622 (4)	4627 (5) *SlA–R;W*	4643 (5) *SlA–R*	*Fe* II; *N* III(?)
		4685 (4)	*He* II 4686
	4705 (4) *SlA–R*	4716 (2)	*He* I
4861 (20)	4861 (20)	4861 (20)	*Hβ*
4927 (3)‡	4902 (5)	4905 (2)	*Fe* II; *He* I
5013 (2)‡	5012 (4) *A–V*	4981 (2)	*Fe* II; *He* I

* About 27 A wide; sharply defined toward violet and uniform in intensity up to $H\gamma$.

† Has apparent absorption in center.

‡ Wave-lengths extrapolated and hence uncertain.

§ The wave-lengths of the hydrogen lines were assumed.

of emission lines and their relative intensities are recorded for each plate separately in Table I. Suggested identifications for the sources of the spectral lines are listed in the last column. *A–R* is designated to mean asymmetrical toward the red; *A–V*, asymmetrical to the violet; *Sl*, slightly; and *W*, very wide. There is a noticeable continuous spectrum on the first plate, a slight amount on the second, and none on the last plate of the series. I have listed only lines which are definitely present. My preliminary note (Harvard Announcement Card No. 278) contained numerous other lines, many of which could not be identified. *Fe* II was identified chiefly with the help of the later plates. Since on two of the plates the spectra were too faint in the violet to record anything except the Balmer Series, the first entry in the table is *H* δ.

CHRISTINE WESTGATE

YERKES OBSERVATORY
WILLIAMS BAY, WIS.
October 1933

REVIEWS

Moderne Physik. By DR. MAX BORN. Prepared for publication by DR. F. SAUTER. Berlin: Julius Springer, 1933. 8vo. Pp. vii+272. RM. 18; bound, RM. 19.50.

In March and April, 1932, Professor Born of the University of Göttingen gave a series of lectures at the Technische Hochschule and the Electrotechnische Verein of Berlin. Dr. Fritz Sauter has, with the help of Dr. Born, prepared the manuscript for publication.

This excellent book consists of seven lectures: (1) "Kinetic Theory of Gases," (2) "Electrical Particles; Protons, Electrons," (3) "Waves and Corpuscles," (4) "Atomic Structure and Line Spectra," (5) "Electron Spin and Pauli Principle," (6) "Quantum Statistics," and (7) "Molecular Structure." An Appendix of sixty-five pages contains mathematical details which were not given during the lectures. O. S.

Bibliographie mensuelle de l'astronomie. Paris: Edited by Société Astronomique de France. Fr. 45.

For the purpose of rapid bibliographic information a committee of the French Astronomical Society, under the chairmanship of A. de la Baume Pluvinel, has inaugurated the publication of a *Bibliographie mensuelle de l'astronomie.*

The first number of this monthly publication is dated March, 1933. It contains the literature received during the preceding month of January by the committee, or by one of the foreign correspondents the help of whom the committee enlisted in order to include publications in all languages. Articles are not abstracted in detail or analyzed critically, but the nature of the contents is mentioned in a few lines so that the reader knows whether the paper is of interest from his special point of view. The subjects are classified under eleven headings, which are further subdivided into paragraphs; in each of the latter the material is presented in alphabetical order of authors. This useful publication does not duplicate in any way the more exhaustive and indispensable *Astronomischer Jahresbericht* which, however, brings information with a delay of a year or more. The yearly subscription of 45 francs for twelve numbers is reduced to 35 francs for members of the Société Astronomique de France, and should be mailed to the secretary, Mr. E. LeRoy, 188 rue du Faubourg Saint-Martin, Paris X^{e} (France). G. V. B.

INDEX TO VOLUME LXXVIII

SUBJECTS

PAGE

Absolute Magnitudes among Stars of Spectral Types A, F, G, and K as Determined from Trigonometric Parallaxes, The Distribution of. *Gustaf Strömberg* 178

7 ε Aurigae, Note on the Spectra of 17 Leporis and. *J. A. Hynek* ' . . 54

Bright Hydrogen Lines, Catalogue and Bibliography of Stars of Classes B and A Whose Spectra Have. *Paul W. Merrill and Cora G. Burwell* 87

Broadening of the Absorption Line *Mg* II λ 4481 in 413 Stars of Class A, A Statistical Study of the Rotational. *Christine Westgate* . . . 46

Calcium Line K, Note concerning the Statistical Relation between Color Excesses and Intensities of the Interstellar. *Christine Westgate* . . 65

27 Canis Majoris, Note on the Radial Velocity of. *J. L. Halpern* . . 64

13 Ceti, The Triple System of. *W. J. Luyten* 225

Classifying Stellar Spectra, The Problem of. *O. Struve* 73

Color Excesses and Intensities of the Interstellar Calcium Line K, Note concerning the Statistical Relation between. *Christine Westgate* . . 65

α Cygni, Variability of Bright *Hα* in. *O. Struve and F. E. Roach* . . 302

Dark Nebulae, Remarks on. *B. P. Gerasimovič* 298

Errors in Trigonometric Parallaxes as a Function of Right Ascension, Systematic. *Adriaan van Maanen* 189

Faculae, A Photometric Study of Sun-Spots and. *R. S. Richardson* . 359

Fission Theory, Some Statistical and Dynamical Aspects of the. *William Markowitz* 161

Hα in α Cygni, Variability of Bright. *O. Struve and F. E. Roach* . . 302

Hagen's Cosmic Clouds, Note on the Sky Brightnesses of Two Regions of. *C. T. Elvey and Paul Rudnick* 156

α_1 Herculis, The Red Titanium Oxide System in. *N. T. Bobrovnikoff* . 211

H.D. 198287–8, Preliminary Report on the Investigation of the System of. *William H. Christie* 200

Hydrogen Lines, Catalogue and Bibliography of Stars of Classes B and A Whose Spectra Have Bright. *Paul W. Merrill and Cora G. Burwell* . 87

Hydrogen Sulphide, On the Spectrum of. *Norman O. Stein* . . . 159

Intensities of Certain Lines of *Ti* II in the Spectra of Three F-Type Stars, On the Relative. *W. W. Morgan* 158

Intensities within a Triplet of *Si* III in Stellar Spectra, Variations in. *C. T. Elvey* 219

17 Leporis and 7 ε Aurigae, Note on the Spectra of. *J. A. Hynek* . . 54

PAGE

Line Intensities, Opacity Formulae and Stellar. *Henry Norris Russell* 239
Magnitude of the Companion of Sirius, The Photovisual. *A. N. Vyssotsky* 1
Magnitudes and an Extension of the Polar Sequence, Systematic Corrections to. *Frederick H. Seares* 141
Nebulae, Remarks on Dark. *B. P. Gerasimovič* 298
Neodymium, Temperature Classification of the Spectrum of. *Arthur S. King* 9
Nova Ophiuchi No. 3, Note concerning the Spectrum of. *Christine Westgate* 372
Opacity Formulae and Stellar Line Intensities. *Henry Norris Russell* . 239
Parallaxes as a Function of Right Ascension, Systematic Errors in Trigonometric. *Adriaan van Maanen* 189
Photometer for the Measurement of Stellar Magnitudes from Photographs, A Modification of the Schilt. *Arthur L. Bennett* . . . 305
Photometric Study of Sun-Spots and Faculae, A. *R. S. Richardson* . . 359
Photometry with the Schraffierkassette. *William H. Christie* . . . 313
Polar Sequence, Systematic Corrections to Magnitudes and an Extension of the. *Frederick H. Seares* 141
Radiation from Variable Stars, Measurements of the. *Edison Pettit and Seth B. Nicholson* 320
Reviews:
Crump, C. C. *The Universe in the Light of Modern Physics* (Max Planck) 223
Elvey, C. T. *The Book of the Sky* (Matthew Luckiesh) 224
Hogness, T. R. *Kinetics of Homogeneous Gas Reactions* (Louis S. Kassel) 69
Morgan, W. W. *Kosmos* (Willem de Sitter) 70
Pogo, A. *Greek Astronomy* (Sir Thomas Heath) 223
Pogo, A. *Trattato di astronomia siderale*, Vol. II: *Le stelle* (Giuseppe Armellini) 71
Rudnick, Paul. *Atom and Cosmos* (Hans Reichenbach) 304
Struve, O. *Lehrbuch der Astronomie* (Elis Strömgren and Bengt Strömgren) 222
Struve, O. *Moderne Physik* (Max Born and Fritz Sauter) 374
Van Biesbroeck, G. *Bibliographie mensuelle de l'astronomie* (Société Astronomique de France) 374
Van Biesbroeck, G. *Tafeln für die Differenzenrechnung sowie für die Hyperbel-, Besselschen, elliptischen und anderen Funktionen* (Keiichi Hayashi) 72
Rotational Broadening of the Absorption Line *Mg* II λ 4481 in 413 Stars of Class A, A Statistical Study of the. *Christine Westgate* . . . 46
Schilt Photometer for the Measurement of Stellar Magnitudes from Photographs, A Modification of the. *Arthur L. Bennett* 305

PAGE

Schraffierkassette, Photometry with the. *William H. Christie* . . . 313
Si III in Stellar Spectra, Variations in Intensities within a Triplet of. *C. T. Elvey* . . . 219
Sirius, The Photovisual Magnitude of the Companion of. *A. N. Vyssotsky* 1
Sky Brightnesses of Two Regions of Hagen's Cosmic Clouds, Note on the. *C. T. Elvey and Paul Rudnick* . . . 156
Spectrum of Nova Ophiuchi No. 3, Note concerning the. *Christine Westgate* . . . 372
Stellar Spectra, The Problem of Classifying. *O. Struve* . . . 73
Sun-Spots and Faculae, A Photometric Study of. *R. S. Richardson* . 359
Ti II in the Spectra of Three F-Type Stars, On the Relative Intensities of Certain Lines of. *W. W. Morgan* . . . 158
Titanium Oxide System in α_1 Herculis, The Red. *N. T. Bobrovnikoff* . 211
Titanium Oxide and Zirconium Oxide Bands in Stellar Spectra, The. *R. S. Richardson* . . . 354
Variable Stars, Measurements of the Radiation from. *Edison Pettit and Seth B. Nicholson* . . . 320
Variable Stars, Request for Unpublished Observations of. *H. Grouiller* . 160
Zirconium Oxide Bands in Stellar Spectra, The Titanium Oxide and. *R. S. Richardson* . . . 354

INDEX TO VOLUME LXXVIII

AUTHORS

PAGE

BENNETT, ARTHUR L. A Modification of the Schilt Photometer for the Measurement of Stellar Magnitudes from Photographs . . . 305

BOBROVNIKOFF, N. T. The Red Titanium Oxide System in α_1 Herculis . 211

BURWELL, CORA G., and PAUL W. MERRILL. Catalogue and Bibliography of Stars of Classes B and A Whose Spectra Have Bright Hydrogen Lines 87

CHRISTIE, WILLIAM H. Photometry with the Schraffierkassette . . 313

CHRISTIE, WILLIAM H. Preliminary Report on the Investigation of the System of H.D. 198287–8 200

CRUMP, C. C. Review of: *The Universe in the Light of Modern Physics*, Max Planck 223

ELVEY, C. T. Review of: *The Book of the Sky*, Matthew Luckiesh . . 224

ELVEY, C. T. Variations in Intensities within a Triplet of *Si* III in Stellar Spectra 219

ELVEY, C. T., and PAUL RUDNICK. Note on the Sky Brightnesses of Two Regions of Hagen's Cosmic Clouds 156

GERASIMOVIČ, B. P. Remarks on Dark Nebulae 298

GROUILLER, H. Request for Unpublished Observations of Variable Stars 160

HALPERN, J. L. Note on the Radial Velocity of 27 Canis Majoris . . 64

HOGNESS, T. R. Review of: *Kinetics of Homogeneous Gas Reactions*, Louis S. Kassel 69

HYNEK, J. A. Note on the Spectra of 17 Leporis and 7 ϵ Aurigae . . 54

KING, ARTHUR S. Temperature Classification of the Spectrum of Neodymium 9

LUYTEN, W. J. The Triple System of 13 Ceti 225

MARKOWITZ, WILLIAM. Some Statistical and Dynamical Aspects of the Fission Theory 161

MERRILL, PAUL W., and CORA G. BURWELL. Catalogue and Bibliography of Stars of Classes B and A Whose Spectra Have Bright Hydrogen Lines 87

MORGAN, W. W. On the Relative Intensities of Certain Lines of *Ti* II in the Spectra of Three F-Type Stars 158

MORGAN, W. W. Review of: *Kosmos*, Willem de Sitter 70

NICHOLSON, SETH B., and EDISON PETTIT. Measurements of the Radiation from Variable Stars 320

PETTIT, EDISON, and SETH B. NICHOLSON. Measurements of the Radiation from Variable Stars 320

PAGE

POGO, A. Review of: *Greek Astronomy*, Sir Thomas L. Heath . . . 223
POGO, A. Review of: *Trattato di astronomia siderale*, Vol. II: *Le stelle*, Giuseppe Armellini 71
RICHARDSON, R. S. A Photometric Study of Sun-Spots and Faculae . 359
RICHARDSON, R. S. The Titanium Oxide and Zirconium Oxide Bands in Stellar Spectra 354
ROACH, F. E., and O. STRUVE. Variability of Bright *Hα* in α Cygni . 302
RUDNICK, PAUL. Review of: *Atom and Cosmos*, Hans Reichenbach . 304
RUDNICK, PAUL, and C. T. ELVEY. Note on the Sky Brightnesses of Two Regions of Hagen's Cosmic Clouds 156
RUSSELL, HENRY NORRIS. Opacity Formulae and Stellar Line Intensities 239
SEARES, FREDERICK H. Systematic Corrections to Magnitudes and an Extension of the Polar Sequence 141
STEIN, NORMAN O. On the Spectrum of Hydrogen Sulphide . . . 159
STRÖMBERG, GUSTAF. The Distribution of Absolute Magnitudes among Stars of Spectral Types A, F, G, and K as Determined from Trigonometric Parallaxes 178
STRUVE, O. The Problem of Classifying Stellar Spectra 73
STRUVE, O. Review of: *Lehrbuch der Astronomie*, Elis Strömgren and Bengt Strömgren 222
STRUVE, O. Review of: *Moderne Physik*, Max Born and Fritz Sauter . 374
STRUVE, O., and F. E. ROACH. Variability of Bright *Hα* in α Cygni . 302
VAN BIESBROECK, G. Review of: *Bibliographie mensuelle de l'astronomie*, Société Astronomique de France 374
VAN BIESBROECK, G. Review of: *Tafeln für die Differenzenrechnung sowie für die Hyperbel-, Besselschen, elliptischen und anderen Funktionen*, Keiichi Hayashi 72
VAN MAANEN, ADRIAAN. Systematic Errors in Trigonometric Parallaxes as a Function of Right Ascension 189
VYSSOTSKY, A. N. The Photovisual Magnitude of the Companion of Sirius 1
WESTGATE, CHRISTINE. Note concerning the Spectrum of Nova Ophiuchi No. 3 372
WESTGATE, CHRISTINE. Note concerning the Statistical Relation between Color Excesses and Intensities of the Interstellar Calcium Line K 65
WESTGATE, CHRISTINE. A Statistical Study of the Rotational Broadening of the Absorption Line *Mg* II λ 4481 in 413 Stars of Class A . . 46

ERRATA

Vol. **78,** No. 2, September, 1933, "Catalogue and Bibliography of Stars of Classes B and A Whose Spectra Have Bright Hydrogen Lines," by Paul W. Merrill and Cora G. Burwell:

Page 100, Notes to Tables I and II, MWC 9, γ Cassiopeiae, and MWC 16, ϕ Persei, and

Page 106, Notes to Tables I and II, MWC 306, β Lyrae: on both pages for *omitted from Table I* read *otherwise omitted from the bibliography, page 114, and the key, page 110.*

Pages 110 ff., Key to Bibliography: No references are available for stars Nos. 95, 279, 335, 391, 405, although this may not be clear from the typography.